International Journal of Electrical and Power Engineering 4 (2): 113-146, 2010
ISSN: 1990-7958

Novel Low Cost Green Plug Smart Filter Soft Starter (GP-SF-SS) Schemes for Small Horse Power Motorized Loads

Adel M. Sharaf and Adel A.A. El-Gammal
Centre for Energy Studies, University of Trinidad and Tobago (UTT),
Wallerfield, Trinidad and Tobago

Abstract: The study presents a family of novel switched smart filter compensated devices using Green Plug Smart Filter Soft Starter (GP-SF-SS) devices for small single phase induction motors used in air-conditioning, ventilation and water pumping. GP-SF-SS devices are members of a family of smart switched filter capacitor compensation devices developed by Sharaf for energy conservation and enhanced utilization of cyclical and temporal type motorized loads. GP-SF-SS devices are equipped with a dynamic online error driven optimally tuned controller that ensures improved power factor, reduced feeder losses, stabilized voltage, minimal current ripples and efficient energy utilization/conservation with minimal impact on the host electric grid security and reliability. The proposed schemes can enhance the power quality; extend induction motor life span by reducing overheating due to inrush currents and harmonics. They prevent overheating and possible motor damage. The family of GP-SF-SS schemes is intended for use with residential/commercial motor drives used in water pumping, ventilation, air conditioning, compressors, refrigeration applications. The family of Green Energy devices and filters is based on concept of avoiding cyclical variations and transients in voltage and current to ensure uniform quasi steady state power and energy load demand.

Key words: Efficiency optimization, energy conservation, Single-Phase Induction Motors Drives (SPIMs), power quality, switched/modulated power filters, Multi Objective Optimization (MOO), Particle Swarm Optimization (PSO), Genetic Algorithm (GA)

INTRODUCTION

Small scale induction motors drives consume over 50% of the total electrical energy generated in the developed countries (Zahedi and Veaz-Zadeh, 2009). The electric utility industry and consumers of electrical energy around the world are facing new challenges for cutting electric energy cost, improving energy utilization, enhancing energy-efficiency, demand-side management, improving supply waveform-power quality, reducing safety hazards to personnel and protecting sensitive computer and automatic-data processing networks (Mademlis *et al*., 2005; De Rossiter Correa *et al*., 2004).

There is a mushrooming use of nonlinear electric loads especially in large motor drives arc furnaces and power electronic converter loads. All these nonlinear loads are byproduct of analog (saturation or limiter type) or digital (converter, solid state switching type) nonlinearities (Shenoy and Nirody, 2006; Neri *et al*., 2005). Nonlinear type loads cause severe waveform distortion, power quality problems interference and extra feeder losses due to excessive inrush currents and severe voltage sags. The extended use of power electronic switching conveners and devices in motor drives, process-industries: Mining. Oil and Gas Industries and industrial DC and AC arc type furnaces have resulted in a polluted grid and unreliable radial distribution/utilization system with serious inherent voltage and power quality problems (Sharaf *et al*., 1998, 2000). These non-linear type electric loads are used with ventilation, air conditioning, water pumping and low power factor industries such as sewing, printing, shear and press machinery and food processing plants.

These non-linear loads also fall in the category of inrush or arc type motorized loads and combined with fluorescent lighting can cause waveform distortion, harmonic interference and voltage flickering (Sharaf and Kreidi, 2002; Sharaf and Chalet, 1998). Generally, direct online motor starting is an economical method for starting induction motors. But direct starting will result in severe voltage sags and extra heating.

When starting large induction motors, excessive voltage dips result in overheating and loss of motor life expectancy (Sharaf and Aljankawey, 2006). In the study, a family of novel switched filter devices using Green Plug Smart Filter Soft Starter (GP-SF-SS) devices equipped with

Corresponding Author: Adel M. Sharaf, Centre for Energy Studies, University of Trinidad and Tobago (UTT), Wallerfield, Trinidad and Tobago

a dynamic online error driven and optimally tuned controllers that can ensure improved power factor, reduced feeder losses, reduced voltage and current ripples, efficient energy utilization/conservation with minimal impact on the electric grid security and supply continuity for single phase induction motor loads. In this study, seven different control strategies were examined and validated, namely: self tuned conventional pid controller, self tuned modified pid controller-I, self tuned modified pid controller-II, self tuned variable structure sliding mode controller vsc/smc/b-b, self tuned zonal activation or target practice controller, self tuned tan-sigmoid incremental integral action controller and self tuned multi-stage incremental action controller.

The need for an on-line gains adaptation or self tunable control mechanism is highly needed in the control of any non-linear systems with un-modeled dynamics. Several AI-related soft computing techniques, such as Genetic Algorithms and Particle Swarm Optimization PSO are emerging as valuable, robust, simple and effective tools in industrial process automation and on-line control adaptation. GA is an iterative search algorithm based on natural selection and genetic search mechanism. However, GA is very fussy; it contains selection, copy, crossover and mutation scenarios and so on. Furthermore, the process of coding and decoding not only impacts its precision but also increases the complexity of the genetic algorithm.

However, Particle Swarm Optimization (PSO) is a novel emerging intelligence which was flexible optimization algorithm proposed in 1995. There are many common characteristics between PSO and GA. First, they are both flexible optimization technologies. Second, they all have strong universal property independent of any gradient information.

However, PSO is much simpler to implement than GA and its operation is more convenient, without selection, copy and crossover. The proposed tri-loop dynamic error driven self tuned controllers are also used to ensure energy efficiency, control loop decoupling, stability and system efficient utilization while maintaining full voltage stability capability. The study presents a novel application of both Multi Objective Particle Swarm Optimization MOPSO and Genetic search Algorithms MOGA optimization and search techniques for online tuning are used to optimally tune the gains of the different controllers.

The smart filter/energy conservation devices ensure for single phase induction motor loads: supply power quality PQ enhancement, enhanced electric energy efficiency, dynamic minimum current ripple tracking, dynamic minimum current level, dynamic minimum power tracking, dynamic minimum effective power ripple tracking, dynamic minimum RMS source current tracking, dynamic maximum power factor, minimum harmonic ripple content, reduced harmonic ripple content, reduction of voltage sags conditions associated with induction motor starting and inrush currents, extended life span of the induction motor, reduced KWh consumption and electricity billing, minimized switching transients and load excursions, maximized power/energy utilization nder unbalanced load conditions, Reduce THD, regulate voltage to be maintained at around 1pu.

MATERIALS AND METHODS

Genetic Algorithm (GA): Genetic algorithm is an optimization method inspired by Darwin's reproduction and survival of the fittest individual (Davis, 1991). This algorithm looks for the fittest individual from a set of candidate solutions called population. The population is exposed to crossover, mutation and selection operators to find the fittest individual. The fitness function assesses the quality of each individual in evaluation process. The selection operator ensures the fittest individuals for the next generation.

The crossover and mutation operators are used for variety of populations. Figure 1 shows the general flow chart of the GA algorithm based on total error iterative minimum search. The steps of genetic algorithm are depicted as follows:

Start: Generate random population of n chromosomes (suitable solutions for the problem).

Fitness: Evaluate the fitness f(x) of each chromosome x in the population.

New population: Create a new population by repeating following steps until the new population is complete:

- Selection: Select two parent chromosomes from a population according to their fitness (the better fitness, the bigger chance to be selected)
- Crossover: With a crossover probability cross over the parents to form a new offspring (children). If no crossover was performed, offspring is an exact copy of parents
- Mutation: With a mutation probability mutate new offspring at each locus (position in chromosome)
- Accepting: Place new offspring in a new population

Replace: Use new generated population for a further run of algorithm.

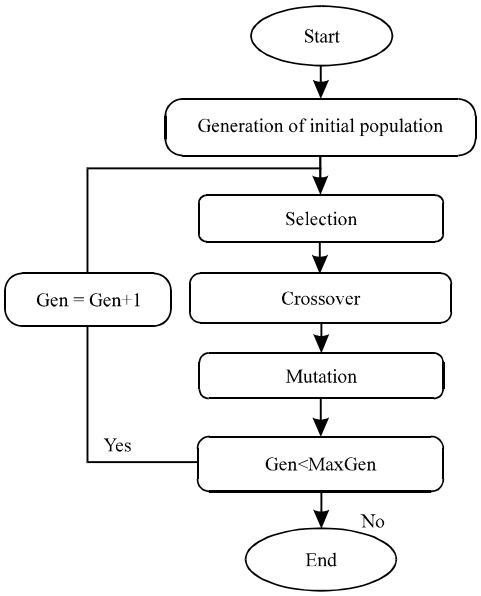

Fig. 1: Flow chart for the GA minimizing search algorithm

Test: If the end condition is satisfied, stop and return the best solution in current population.

Loop: Go to step 2.

Particle swarm optimization: Particle Swarm Optimization (PSO) is an evolutionary computation optimization technique (a search method based on a natural system) developed by Kennedy and Eberhart (1995) and Shi and Eberhart (1999).

The system initially has a population of random selective solutions. Each potential solution is called a particle. Each particle is given a random velocity and is flown through the problem space. The particles have memory and each particle keeps track of its previous best position (called the P_{best}) and its corresponding fitness. There exist a number of P_{best} for the respective particles in the swarm and the particle with greatest fitness is called the global best (G_{best}) of the swarm. The basic concept of the PSO technique lies in accelerating each particle towards its P_{best} and G_{best} locations with a random weighted acceleration at each time step. The main steps in the particle swarm optimization algorithm and selection process are described as follows:

- Step 1: Initialize a population of particles with random positions and velocities in d dimensions of the problem space and fly them
- Step 2: Evaluate the fitness of each particle in the swarm
- Step 3: For every iteration, compare each particle's fitness with its previous best fitness (P_{best}) obtained. If the current value is better than P_{best}, then set P_{best} equal to the current value and the P_{best} location equal to the current location in the d-dimensional space
- Step 4: Compare P_{best} of particles with each other and update the swarm global best location with the greatest fitness (G_{best})
- Step 5: Change the velocity and position of the particle

According to Eq. 1 and 2, respectively

$$V_{id} = \omega \times V_{id} + C_j \times rand_1 \times (P_{id} - X_{id}) + C_2 \times rand_2 \times (P_{gd} - X_{id}) \quad (1)$$

$$X_{id} = X_{id} + V_{id} \quad (2)$$

Where V_{id} and X_{id} represent the velocity and position of the ith particle with d dimensions, respectively. $rand_1$ and $rand_2$ are two uniform random functions and ω is the inertia weight which is chosen beforehand.

- Repeat steps 2-5 until convergence is reached based on some desired single or multiple criteria

The PSO optimization search utilized dynamic total error minimization algorithm has many key parameters and these are described as follows: ω is called the inertia weight that controls the exploration and exploitation of the search space because it dynamically adjusts velocity. V_{max} is the maximum allowable velocity for the particles (i.e., in the case where the velocity of the particle exceeds V_{max} then it is limited to V_{max}). Thus, resolution and fitness of search depends on V_{max}. If V_{max} is too high then particles will move beyond a good solution. If V_{max} is too low, particles will be trapped in local minima. The constants C_1 and C_2 in Eq. 1 and 2, termed as cognition and social components, respectively. These are the acceleration constants which changes the velocity of a particle towards P_{best} and G_{best} (generally, somewhere between P_{best} and G_{best}). Figure 2 shows the general flow chart of the PSO algorithm based on total error iterative minimum search. The most striking difference between PSO and the other evolutionary algorithms is that PSO chooses the path of cooperation over competition.

The other optimization algorithms commonly use some form of decimation, survival of the fittest. In contrast, the PSO population is stable and individuals are not destroyed or recreated. Individuals are influenced by the best performance of their neighbors. Individuals eventually converge on optimal points in the problem domain. In addition, the PSO traditionally does not have genetic operators like crossover between individuals and

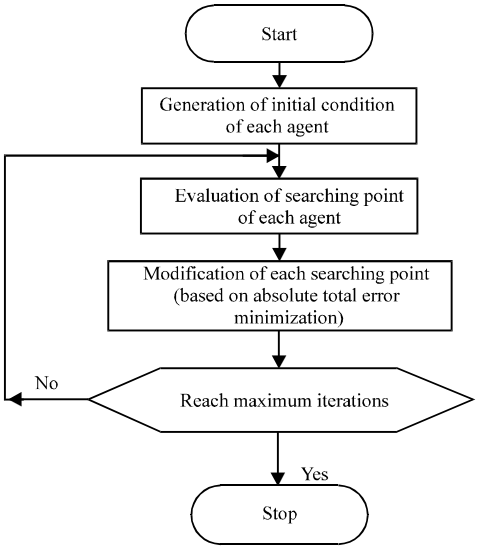

Fig. 2: Flow chart for the PSO minimizing search algorithm

mutation and other individuals never substitute particles during the run. So, in PSO all the particles tend to converge to the best solution quickly, comparing with GA.

Multiobjective optimization: The following definitions are used in the proposed Multi Objective Optimization (MOO) search algorithm (Ngatchou *et al*., 2005; Berizzi *et al*., 2001; Coello and Lechuga, 2002).

Defination 1: The general MO problem requiring the optimization of N objectives may be formulated as follows:

$$\vec{y} = \vec{F}(\vec{x}) = [\vec{f}_1(\vec{x}), \vec{f}_2(\vec{x}), \vec{f}_3(\vec{x}), \ldots \vec{f}_N(\vec{x})]^T \quad (3)$$

$$\text{subject to } g_j(x) \le 0 \qquad j = 1, 2, \ldots, M \quad (4)$$

$$\vec{x}^* = [\vec{x}_1^*, \vec{x}_2^*, \ldots, \vec{x}_P^*]^T \in \Omega \quad (5)$$

Where:

$\vec{y}$ = The objective vector

$g_j(\vec{x})$ = Represents the constraints

$\vec{x}$ = P-dimensional vector representing the decision variables within a parameter space Ω

The space spanned by the objective vectors is called the objective space. The subspace of the objective vectors satisfying the constraints is called the feasible space.

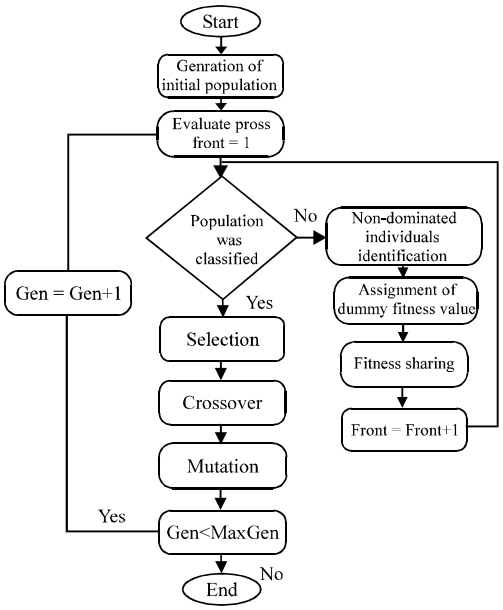

Fig. 3: Flow chart of NSGA

Defination 2: A decision vector $\vec{x}_1 \in \Omega$ is said to dominate the decision vector $\vec{x}_2 \in \Omega$ (denoted by) $\vec{x_1} \prec \vec{x_2}$, if the decision vector $\vec{x}_1$ is not worse than $\vec{x}_2$ in all objectives and strictly better than $\vec{x}_2$ in at least one objective.

Defination 3: A decision vector $\vec{x}_1 \in \Omega$ is called Pareto-optimal, if there does not exist another $\vec{x}_2 \in \Omega$ that dominates it. An objective vector is called Pareto-optimal, if the corresponding decision vector is Pareto-optimal.

Defination 4: The non-dominated set of the entire feasible search space Ω is the Pareto-optimal set. The Pareto-optimal set in the objective space is called Pareto-optimal front.

Multi-objective genetic algorithm: The Non-dominated Sorting Genetic Algorithm (NSGA) is a multi-objective genetic algorithm that was developed by Deb *et al*. (2002). This algorithm has been chosen over a conventional genetic algorithm for three principal reasons: no need to specify a sharing parameter, a strong tendency to find a diverse set of solutions along the Pareto optimal front and the ability to specify multiple objectives without the need to combine them using a weighted sum. The basic idea behind NSGA is the ranking process executed before the selection operation, as shown in Fig. 3. This process identifies non dominated solutions in the population, at each generation to form non dominated fronts (Srinivas and Deb, 1994), after this the selection, crossover and mutation usual operators are performed. In the ranking

procedure, the non dominated individuals in the current population are first identified. Then, these individuals are assumed to constitute the first non dominated front with a large dummy fitness value (Srinivas and Deb, 1994).

The same fitness value is assigned to all of them. In order to maintain diversity in the population, a sharing method is then applied. Afterwards, the individuals of the first front are ignored temporarily and the rest of population is processed in the same way to identify individuals for the second non dominated front.

A dummy fitness value that is kept smaller than the minimum shared dummy fitness of the previous front is assigned to all individuals belonging to the new front. This process continues until the whole population is classified into non dominated fronts. Since the non dominated fronts are defined, the population is then reproduced according to the dummy fitness values.

Multi-objective particle swarm optimization: In MOPSO (Ngatchou *et al*., 2005; Berizzi *et al*., 2001; Coello and Lechuga, 2002), a set of particles are initialized in the decision space at random. For each particle i, a position x_i in the decision space and a velocity v_i are assigned. The particles change their positions and move towards the so far best-found solutions.

The non-dominated solutions from the last generations are kept in the archive. The archive is an external population in which the so far found non-dominated solutions are kept. Moving towards the optima is done in the calculations of the velocities as follows:

$$V_{id} = \omega \times V_{id} + C_1 \times rand_1 \times (P_{pd} - X_{id}) + C_2 \times rand_2 \times (P_{rd} - X_{id}) \quad (6)$$

Where:

$P_{r,d}$, $P_{p,d}$ = Randomly chosen from a single global Pareto archive

ω = Inertia factor influencing the local and global abilities of the algorithm

$V_{i,d}$ = The velocity of the particle i in the dth dimension

c_1 and c_2 = Weights affecting the cognitive and social factors, respectively

r_1 and r_2 = Uniform random functions in the range (Zahedi and Veaz-Zadeh, 2009)

According to Eq. 6, each particle has to change its position $X_{i,d}$ towards the position of the two guides $P_{r,d}$, $P_{p,d}$ which must be selected from the updated set of non-dominated solutions stored in the archive. The particles change their positions during generations until a termination criterion is met. Finding a relatively large set of Pareto-optimal trade-off solutions is possible by running the MOPSO for many generations. Figure 4 shows the flow chart of the Multi-Objective Particle Swarm Optimization MOPSO.

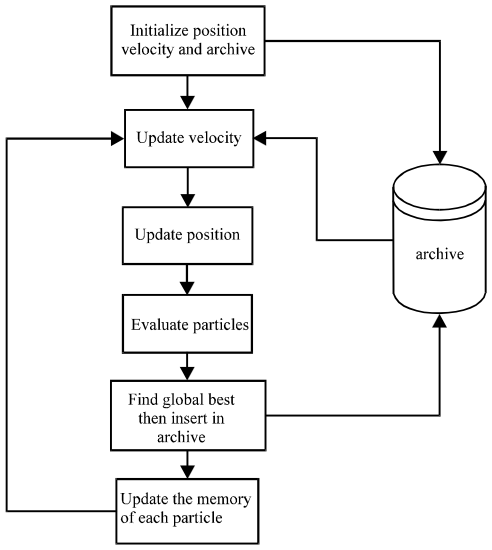

Fig. 4: Flow chart of the MOPSO optimization search algorithm

RESULTS AND DISCUSSION

PSO and other Evolutionary Computation (EC) techniques: A comparison between conventional optimization techniques and evolutionary algorithms (like genetic algorithm and PSO) is shown in Table 1 (Poirier *et al*., 2001). The most striking difference between PSO and the other evolutionary algorithms is that PSO chooses the path of co-operation over competition.

The other algorithms commonly use some form of decimation, survival of the fittest. In contrast, the PSO population is stable and individuals are not destroyed or created. Individuals are influenced by the best performance of their neighbors. Individuals eventually converge on optimal points in the problem domain. In addition, the PSO traditionally does not have genetic operators like crossover between individuals and mutation and other individuals never substitute particles during the run. Instead the PSO refines its search by attracting the particles to positions with good solutions. Moreover, compared with genetic algorithms (GAs), the information sharing mechanism in PSO is significantly different. In GAs, chromosomes share information with each other.So the whole population moves like a one group towards an optimal area. In PSO, only Gbest (or Pbest) gives out the information to others. It is a one-way information sharing mechanism. The evolution only looks

Table 1: comparison between conventional optimization procedures and evolutionary algorithms

Property	Evolutionary	Traditional
Search space	Population of potential solutions	Trajectory by a single point
Motivation	Natural selection and social adaptation	Mathematical properties (gradient, Hessian)
Applicability	Domain independent, applicable to variety of problems	Applicable to a specific problem domain
Point transition	Probabilistic	Deterministic
Prerequisites	An objective function to be optimised	Auxiliary knowledge such as gradient vectors
Initial guess	Automatically generated by the algorithm	Provided by user
Flow of control	Mostly parallel	Mostly serial
CPU time	Large	Small
Results	Global optimum more probable	Local optimum, dependant of initial guess
Advantages	Global search, parallel, speed	Convergence proof
Drawbacks	No general formal convergence proof	Locality, computational cost

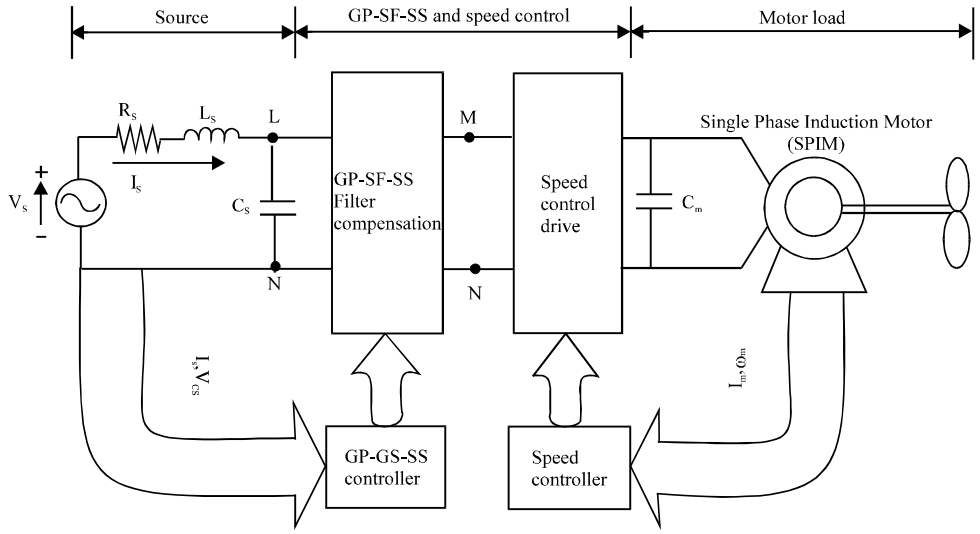

Fig. 5: The proposed Green Plug-Smart Filter-Soft Starter (GP-SF-SS) for Single Phase Induction Motor (SPIM) drive system

for the best solution. In PSO all the particles tend to converge to the best solution quickly, comparing with GA, even in the local version in most cases.

Sample study motorized system: Figure 5 shows the block diagram of the utilization Single-phase Induction Motor (SPIM) and the connection of the Green Plug-Smart Filter-Soft Starter (GP-SF-SS) and the speed control drive system to the SPIM load. Figure 6 and 7 show the proposed tri-loop dynamic tracking controller to ensure both objectives of (energy/power) saving as well as power quality enhancement of the supply system current and load bus voltage.

The novel PSO and GA self tuned multi regulators and coordinated controller are used for the following purposes: Green Plug Filter Compensator GPFC-SPWM regulator for pulse width switching scheme to regulate the DC bus voltage and minimize inrush current transients and load excursions and the SPIM drive with the speed regulator that ensure speed reference tracking with minimum inrush conditions and ensure reduced voltage transients and improved energy utilization. Figure 8 and 15 show the proposed family of Green Plug-Smart Filter-Soft Starter (GP-SF-SS) schemes.

Figure 8 shows a hybrid series, parallel filter compensator scheme acting as a series/parallel capacitor and or parallel tuned arm filter. Figure 9 shows a switched capacitor compensator scheme with combined parallel tuned arm filter.

Figure 10 shows a hybrid switched series/parallel capacitor compensation scheme which acts with AC source and SPIM inductances as a blocking tuned arm filter. Figure 11 shows a combined capacitor compensator or tuned arm filter.

Figure 12 shows a switched series and/or parallel capacitor compensator for series compensation and power factor correction. Figure 13 shows a switched doubly tuned arm filter at two separate tuned frequencies. Figure

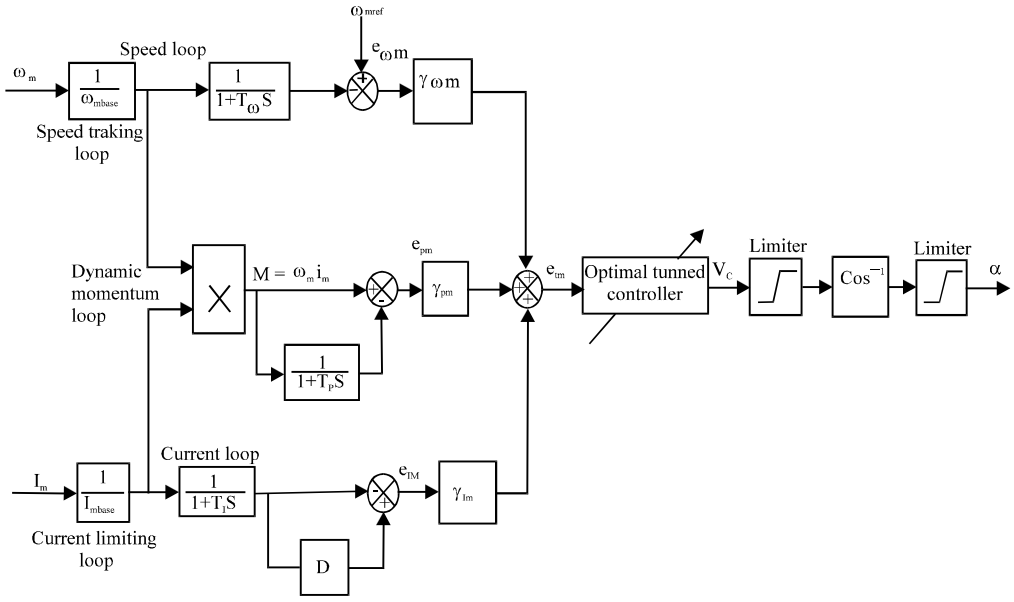

Fig. 6: Tri-loop error driven self regulating dynamic controller for control of Single Phase Induction Motor (SPIM) drive

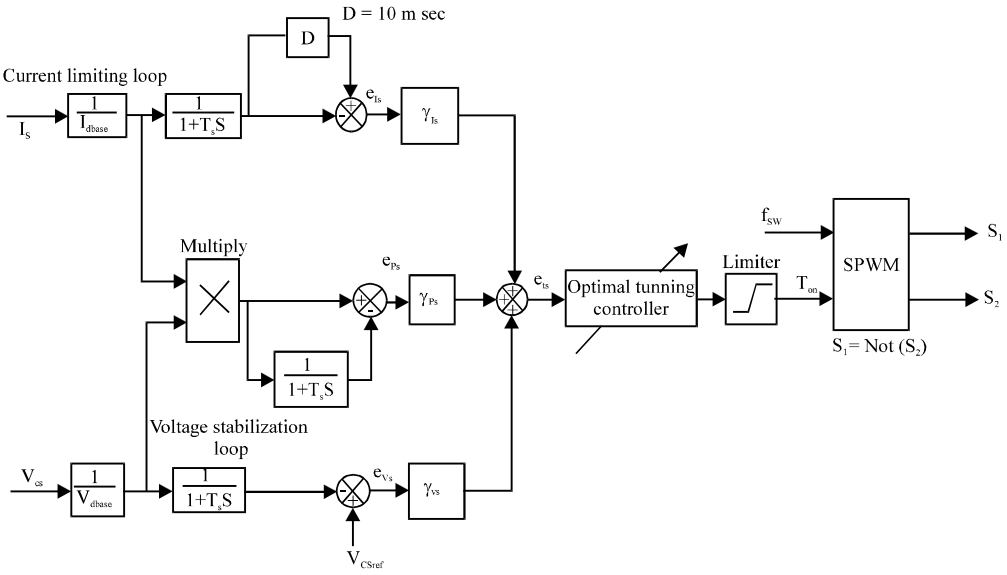

Fig. 7: Tri-loop error driven self regulating dynamic controller for the Green Plug-Smart Filter–Soft Starter (GP-SF-SS) scheme

14 shows a switched tuned arm filter using a low cost triac. Finally, Fig. 15 shows a switched C-type damped power filter capable of providing a low impedance path to all harmonics. It can utilize a triac or a fast MOSFET switch in slow and fast dynamic loads.

All filters objectives can be either: harmonic reduction and Power Quality (PQ) enhancement or electric power/energy savings and dynamic reactive compensation for the single phase induction motor loads. The proposed utilization scheme is fully validated using the Matlab/Simulink software environment under normal conditions, load excursion, SPIM motor torque changes to assess the control system robustness, effective energy utilization and speed reference tracking.The common concerns of power quality are the long duration voltage variations (overvoltage, under-voltage and sustained

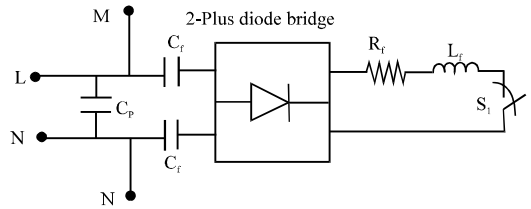

Fig. 8: Economic tuned-arm power filter and capacitor compensator scheme-A

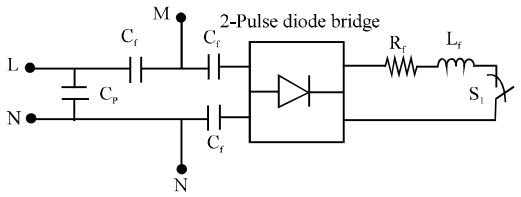

Fig. 9: Low cost tuned-arm power filter/capacitor compensator scheme-B

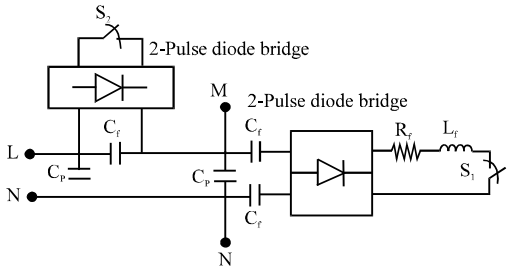

Fig. 10: Low cost tuned-arm power filter and capacitor compensation scheme-C

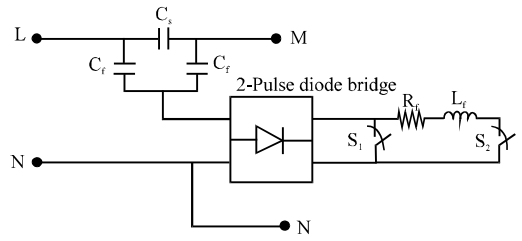

Fig. 11: Low cost tuned-arm power filter/capacitor compensator scheme-D

interruptions), short duration voltage variations (interruption, sags and swells), voltage imbalance (voltage unbalance), waveform distortion (DC offset, harmonics, inter-harmonics, notching and noise), voltage fluctuation (voltage flicker) and power frequency variations. To prevent the undesirable states and to reduce the power consumption, a GPF scheme is used to stabilize system.

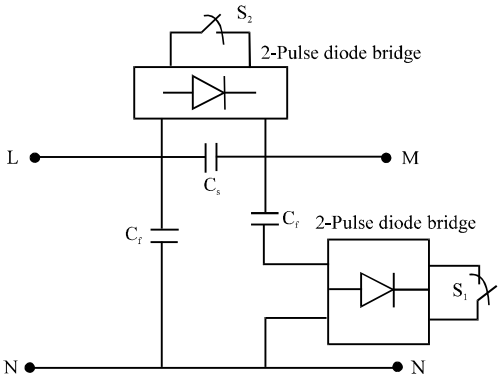

Fig. 12: Switched series parallel capacitor compensator scheme-E

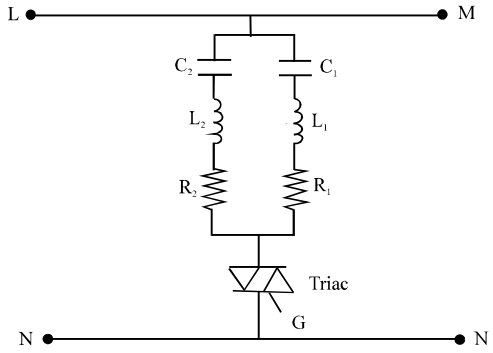

Fig. 13 Dual-tuned-arm filter compensator scheme-F

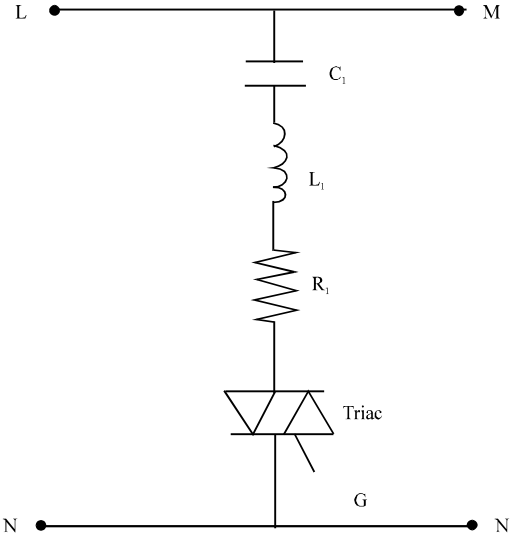

Fig. 14: Low cost Tuned-Arm Power Filter (TAF) compensator scheme-G

Dynamic error driven control: The proposed control system comprises two sub-regulators or controllers

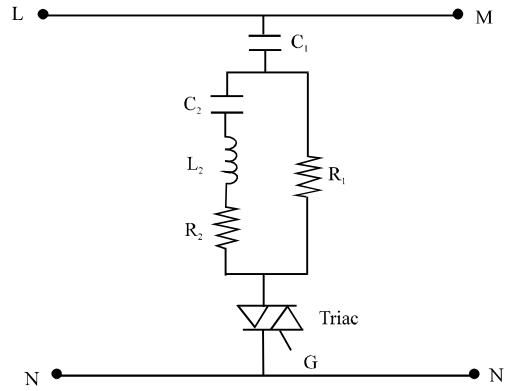

Fig. 15: Low cost switched C-type power filter compensator scheme-H

named as DC side Green Plug Filter Compensator GPFC-SPWM regulator and the SPIM drive speed controller. Figure 6 and 7 depict the proposed multi-loop dynamic self regulating controllers based on multi objective optimization search and optimization technique based on soft computing PSO and GA.

The global error is the summation of the three loop individual errors including voltage stability, current limiting and synthesize dynamic power loops. Each multi loop dynamic control scheme is used to reduce a global error based on a tri-loop dynamic error summation signal and to mainly track a given speed reference trajectory loop error in addition to other supplementary motor current limiting and dynamic power loops are used as auxiliary loops to generate a dynamic global total error signal that consists of not only the main loop speed error but also the current ripple, over current limit and dynamic over load power conditions.

The global error signal is input to the self tuned controllers shown in Fig 6. The (per-unit) three dimensional-error vector (e_{vs}, e_{Is}, e_{ps}) of the electric source controller scheme is governed by the following equations:

$$e_{vs}(k)=V_s(k)\left(\frac{1}{1+ST_s}\right)\left(\frac{1}{1+SD}\right)-V_s(k)\left(\frac{1}{1+ST_s}\right) \quad (7)$$

$$e_{Is}(k)=I_s(k)\left(\frac{1}{1+ST_s}\right)\left(\frac{1}{1+SD}\right)-I_s(k)\left(\frac{1}{1+ST_s}\right) \quad (8)$$

$$e_{Ps}(k)=I_s(k)\times V_s(k)\left(\frac{1}{1+ST_s}\right)\left(\frac{1}{1+SD}\right)-I_s(k)\times V_s(k)\left(\frac{1}{1+ST_g}\right) \quad (9)$$

The total or global error $e_{ts}(k)$ for the GP-SF-SS side scheme at a time instant:

$$e_{ts}(k)=\gamma_{vs}e_{vs}(k)+\gamma_{is}e_{is}(k)+\gamma_{Ps}e_{Ps}(k) \quad (10)$$

In the same manner, the (per-unit) three dimensional-error vector ($e_{\omega m}$, e_{Im}, e_{pm}) of the SPIM motor scheme is governed by the following equations:

$$e_{\omega m}(k)=\omega_m(k)\left(\frac{1}{1+ST_m}\right)\left(\frac{1}{1+SD}\right)-\omega_m(k)\left(\frac{1}{1+ST_m}\right) \quad (11)$$

$$e_{Im}(k)=I_m(k)\left(\frac{1}{1+ST_m}\right)\left(\frac{1}{1+SD}\right)-I_m(k)\left(\frac{1}{1+ST_m}\right) \quad (12)$$

$$e_{Pm}(k)=I_m(k)\times\omega_m(k)\left(\frac{1}{1+ST_m}\right)\left(\frac{1}{1+SD}\right)-I_m(k)\times\omega_m(k)\left(\frac{1}{1+ST_m}\right) \quad (13)$$

And the total or global error e_{tm} (k) for the MPFC scheme at a time instant:

$$e_{tm}(k)=\gamma_{\omega m}e_{\omega m}(k)+\gamma_{im}e_{im}(k)+\gamma_{Pm}e_{Pm}(k) \quad (14)$$

A number of conflicting objective functions are selected to optimize using the PSO algorithm. These functions are defined by the following:

J1 = Minimize the Total Harmonic Distortion of the load current (THDi)
J2 = Minimize the Total Harmonic Distortion of the load Voltage (THDv)
J3 = Maximize the electric energy efficiency
J4 = Maximize the power factor
J5 = Minimize the KWh consumption

In general, to solve this complex optimality search problem, there are two possible optimization techniques based on Particle Swarm Optimization (PSO): Single aggregate selected Objective Optimization (SOO) which is explained and Multi Objective Optimization (MOO). The main procedure of the SOO is based on selecting a single

aggregate objective function with weighted single objective parameters scaled by a number of weighting factors. The objective function is optimized (either minimized or maximized) using either Genetic Algorithm (GA) or Particle Swarm Optimization search algorithm (PSO) methods to obtain a single global or near optimal solution. On the other hand, the main objective of the Multi Objective (MO) problem is finding the set of acceptable (trade-off) optimal solutions. This set of accepted solutions is called Pareto front.

These acceptable trade-off multi level solutions give more ability to the user to make an informed decision by seeing a wide range of near optimal selected solutions that are feasible and acceptable from an overall standpoint. Single Objective (SO) optimization may ignore this trade-off viewpoint which is crucial.

The main advantages of the proposed MOO method are: It doesn't require a priori knowledge of the relative importance of the objective functions and it provides a set of acceptable trade-off near optimal solutions. This set is called Pareto front or optimality trade-off surfaces. Both SOO and MOO searching algorithms are tested, validated and compared.

The dynamic error driven controller regulates the controllers' gains using the Particle Swarm Optimization (PSO) and GA to minimize the system total error and the selected objective functions. The proposed dynamic tri loop error driven controller, developed by Sharaf which is a novel advanced regulation concept that operates as an adaptive dynamic type multi-purpose controller capable of handling sudden parametric changes, load and/or source excursions.

By using the tri loop error driven controller, it is expected to have a smoother, less dynamic overshoot, fast and more robust controller when compared to those of classical control schemes. Seven different control structures were examined and validated, for speed trajectories tracking: tuned conventional PID controller, tuned modified PID controller-I, tuned modified PID controller-II, tuned variable structure sliding mode controller VSC/SMC/B-B, tuned zonal activation or target practice controller, tuned tan-sigmoid incremental integral action controller and tuned multi-stage incremental action controller.

Self tuned conventional PID controller: Fundamentally, the conventional PID controller comprises three basic control actions. They are simple to implement and they provide good performance. The tuning process of the gains of PID controllers can be complex because is iterative: first, it is necessary to tune the proportional mode, then the integral and then add the derivative mode to stabilize the overshoot then add more proportional and so on. The PID controller has the following form in the time domain as shown in Fig. 16:

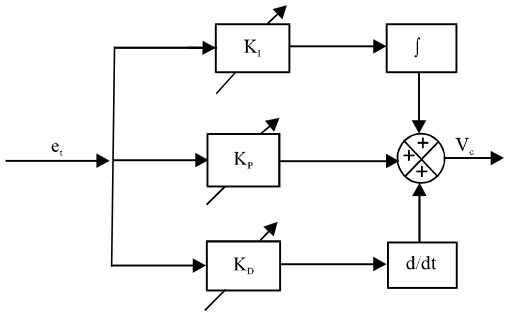

Fig. 16: Optimally tuned conventional PID controller block diagram

$$u(t)= K_p e(t) + K_i \int_0^t e(t)dt + K_d \frac{de(t)}{dt} \qquad (15)$$

Where:

$e(t)$ = The selected system error
$u(t)$ = The control variable
K_p = The proportional gain
K_i = The integral gain
K_d = The derivative gain

Each coefficient of the PID controller adds some special characteristics to the output response of the system. Because of this choosing the right parameters becomes a crucial decision. In this scheme, the tri loop error driven controller is utilized with traditional PID controller. PID controller gains (K_P, K_I, K_D) are dynamically self tuned using the PSO and GA dynamic search and optimization criterion based on total error minimization, steady state error, maximum overshoot, settling time and rising time.

Self tuned modified PID controller-I: In the tuned modified PID controller- I proposed controller scheme, an optimally tuned modified PID controller for the SPIM motor drive systems is developed using the Particle Swarm Optimization technique (PSO) and the Genetic Algorithm GA, where the additional integral of the squared system error is implemented in this modified PID controller as shown in Fig. 17.

$$u(t)= K_p e(t) + K_i \int_0^t e(t)dt + K_d \frac{de(t)}{dt} + K_e \left(e(t)\right)^2 \qquad (16)$$

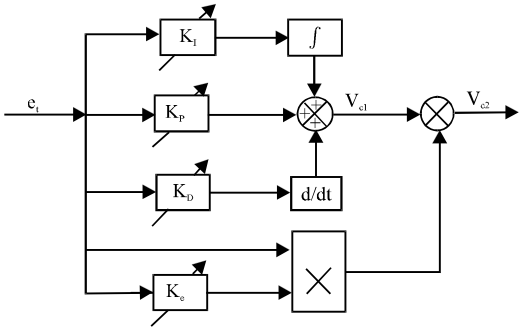

Fig 17: Optimally Tuned modified PID controller- I block diagram

The modified PID controller gains (K_P, K_I, K_D and K_e) are tuned using the PSO searching algorithm to minimize the selected objective functions (J_1-J_5).

Self tuned modified PID controller-II: The tuned modified PID controller–II proposed control scheme is shown in Fig. 18. The resultant control voltage has the form in the time domain as:

$$u(t)=\left(K_P e(t)+K_i\int_0^t e(t)dt+K_d\frac{de(t)}{dt}\right)\times K_e e(t)^2 \tag{17}$$

Self tuned Variable Structure Sliding Mode Bang-Bang (VSC/SMC/B-B) controller: In the variable structure sliding mode controller scheme, an optimally adaptive and self tuned variable structure sliding mode controller for SPIM motor drive systems using Particle Swarm Optimization technique (PSO) and Genetic Algorithm (GA) as shown in Fig 19. The slope of the sliding surface is designed as:

$$\sigma=\beta e_t+K_\alpha\frac{de_t}{dt} \tag{18}$$

With adaptive term:

$$\beta=\beta_0+\beta_1|e_t| \tag{19}$$

Where;

$$|e_t|=\sqrt{(\gamma_I e_I)^2+(\gamma_\omega e_\omega)^2+(\gamma_v e_v)^2+(\gamma_P\gamma_P)^2} \tag{20}$$

The system control voltage has the following form in the time domain (Srinivas and Deb, 1994), the control is an on-off logic that is when $\sigma > 0$, $V_c = 1$ and when $\sigma < 0$, $V_c = -1$.

The PSO and GA optimization and parameters searching algorithms are implemented for tuning the gains β_0, β_1 and α to minimize the selected objective functions (J_1-J_5).

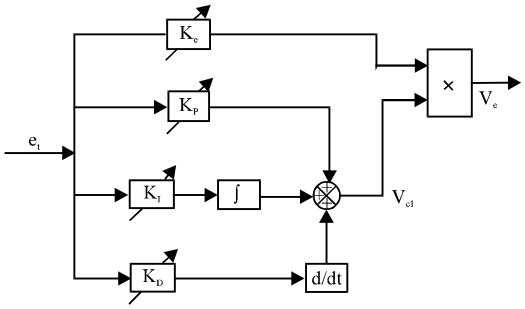

Fig. 18: Optimally tuned modified PID controller-II block diagram

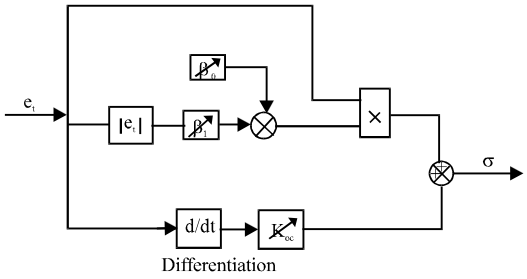

Fig. 19: Optimally tuned VSC/SMC/B-B controller block diagram

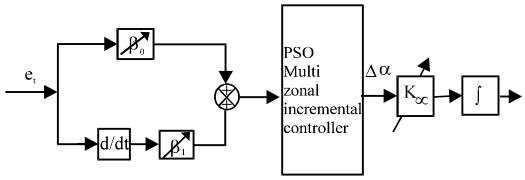

Fig. 20: Optimally tuned zonal activation or target Practice controller block diagram

Self tuned zonal activation or target practice controller: Figure 20 shows the proposed zonal activation or target practice controller scheme. In this strategy, the tri loop error driven controller is utilized with zonal activation or target practice controller which is dynamically self tuned using the PSO and GA search and optimization criterion based on total error minimization, steady state error, maximum overshoot and settling and rising time. The dynamic supplementary control loops utilizes speed, current, ripples and dynamic momentum excursion errors. Zonal Activation Target Practice Controller is composed from concentric circles representative zones, each circle has a radius depends on the values of the total error and the first derivative of the total error as shown in Fig 21:

$$R=\beta_1 e(t)+\beta_0\frac{de(t)}{dt} \tag{21}$$

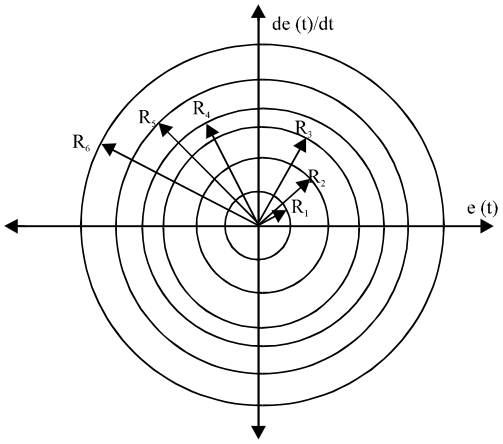

Fig. 21: Zonal activation target practice controller boundaries

Table 2: Zonal activation controller boundaries *number of zones can be selected for best performance

Zone no.	Zone boundary (PU)	Δα (deg)
1	$0 \le R_1 \le 0.025$	2.5
2	$0.025 \le R_2 \le 0.05$	5.0
3	$0.05 \le R_3 \le 0.1$	10.0
4	$0.1 \le R_4 \le 0.2$	20.0
5	$0.2 \le R_5 \le 0.4$	30.0
6	$0.4 \le R_6 \le 0.5$	40.0

Zonal activation target Practice controller determines the value of boundaries Δα which assigned to each zone according to the values of the total error and the first derivative of the total error as shown in Table 2 and Fig. 20. Then the value of the controlling firing angle α is determined using the following form:

$$\alpha = \int K_{\alpha} d\alpha \tag{22}$$

Where $0.01 \le K_{\alpha} \le 1.0$, β_0 and β_1 are an optimization parameter which is tuned using MOPSO and MOGA to minimize the selected objective functions.

Self tuned tan-sigmoid incremental controller: Figure 22 shows the Tan-sigmoid self adjusting multi loop controller. The change in the control voltage ΔV_c is defined as:

$$\Delta V_c = k_0 R_e \left(\frac{1 - e^{-\beta_0 e(t)}}{1 + e^{-\beta_0 e(t)}} \right) \tag{23}$$

Where:

$$R = \sqrt{\left(e(t)\right)^2 + \left(\frac{d}{dt} e(t)\right)^2} \tag{24}$$

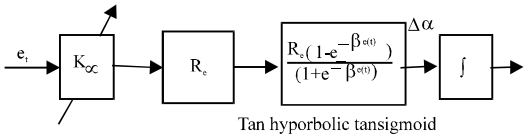

Fig 22: Optimally tuned tan-sigmoid incremental integral action controller

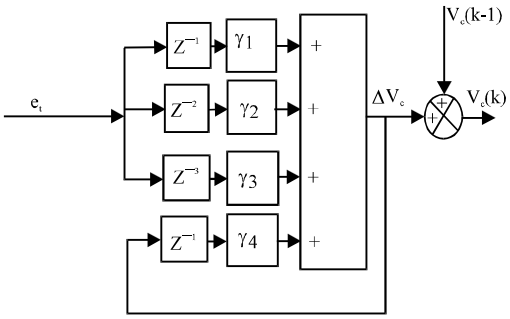

Fig 23: Tuned multi-Stage incremental action regression based controller block diagram

and: $50 \le K_0 \le 200.0$, $1 \le \beta \le 5$ are optimization parameters which are tuned using MOPSO and MOGA to minimize the selected objective functions. The system control voltage has the following form in the time domain:

$$V_c = \int_0^t \Delta V_c dt \tag{25}$$

Self tuned multi-loop incremental controller: Figure 23 shows the change in the control voltage ΔV_c of the Multi-loop incremental controller that is defined as:

$$\Delta V_c(k) = \gamma_1 e(k-1) + \gamma_2 e(K-2) + \gamma_3 e(k-3) + \gamma_4 e(k-4) + \gamma_5 \Delta V_c \tag{26}$$

$$V_c(k) = \Delta V_c(k) + V_c(k-1) \tag{27}$$

In this strategy, the PSO and GA searching algorithms are implemented for tuning the gains (γ_1-γ_4) minimize the selected objective functions (J_1-J_5).

Self tuned Artificial Neural Network controller (ANN): The neural network used in this study is the simplest one that uses three layers which is widely used in the control of the electrical machines. Each layer is composed of neurons. Each neuron is connected via weights to the previous layer. The first layer is connected to the input variables. The second one is connected via weights to all the neurons of the previous layer and the last one is composed of one neuron given the output value. The weights and the biases of the ANN network's are updated

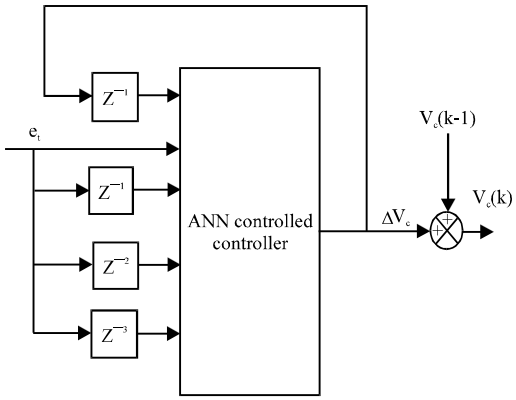

Fig. 24: ANN incremental controlled controller block diagram

to provide that the global error of the system is minimized. The proposed ANN regulator is tuned on-line using the back-propagation algorithm. The on-line ANN rule-based algorithm is used to update the ANN network weights and biases to ensure continuous effective dynamic response while keeping the motor inrush current under specified tolerable limits. The input vector with 3 layer ANN as shown in Fig. 24 is:

$$\overline{X}=\{e_t(k-1),e_t(k-2),e_t(k-3),\Delta V_c(k-1)\} \quad (28)$$

Self tuned Fuzzy Logic Controller (FLC): As shown in Fig. 25, the FLC system consists of three subsystems which are the fuzzification, rule base and defuzzification. Fuzzification subsystem converts the exact inputs to fuzzy values using five membership functions: Positive Big (PB), Positive Small (PS), Zero (ZZ), Negative Small (NS) and Negative Big (NB). The rule base unit processes these fuzzy values with fuzzy rules.

The defuzzification unit converts the fuzzy results to exact values. The FLCs input values are the global error e_t and change in global error, de_t. According to these variables, a rule table is produced in the FLCs rule base unit as shown in Table 3.

Digital simulation results: The GP-SF-SS devices system performance is compared for two cases; without (as shown in Table 4) and with the GP-SF-SS devices, the second case is studied with fixed and self tuned type controllers using either GA or PSO. In addition, the second case is studied to compare the performance with Artificial Neural Network (ANN) controller (Table 5) and Fuzzy Logic Controller FLC (Table 6) with the self tuned type controllers using either GA

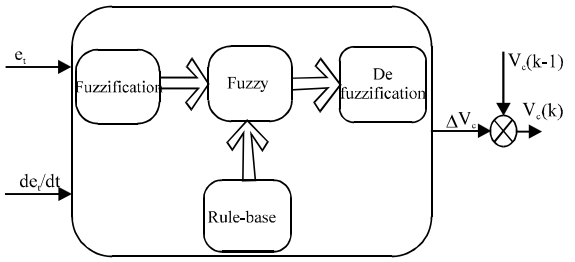

Fig. 25: Main structure of the FLC-incremental controller

Table 3: Fuzzy rules decision table

	de_t				
e_t	NB	NS	ZZ	PS	PB
NB	NB	NB	NS	NS	ZZ
NS	NB	NS	NS	ZZ	PS
ZZ	NS	NS	ZZ	PS	PS
PS	NS	ZZ	PS	PS	PB
PB	ZZ	PS	PS	PB	PB

Table 4: System behavior without (GP-SF-SS) schemes

Items	Without (GP-SF-SS) RMS
RMS motor voltage (PU)	0.8782
RMS motor current (PU)	0.8576
Maximum transient voltage over/under shoot (PU)	0.1597
Maximum transient current-over/under shoot (PU)	0.1775
System efficiency	0.8145
NMSE_V	0.3293
NMSE_ω_m	0.5093
NMSE_I	0.2398
THDv_bus L (%)	17.486
THDi_bus L (%)	19.475
THDv_bus M (%)	16.456
THDi_bus M (%)	18.465
Motor power factor	0.7516

or PSO. The seven self tuned type controllers based either GA or PSO are tuned conventional PID controller, tuned modified PID controller-I, Tuned modified PID controller-II, tuned variable structure sliding mode controller VSC/SMC/B-B, tuned zonal ctivation or target practice controller, tuned tan-sigmoid incrementali integral action controller and tuned multi-stage incremental action controller.

All of the controllers discussed in the study have been applied to the speed tracking control of the same system parameters for performance comparison. Matlab-Simulink Software was used to design, test and validate the effectiveness of the GP-SF-SS devices for small motors used in household appliances, washers, dryers, fans, water pumps, ventilation systems, air-conditions and other applications in dispersing machines, actuators and small converters with induction motor size up to 5-25 KVA. The digital dynamic simulation model using Matlab/Simulink software environment allows for low cost

Table 5: System dynamic behavior comparison using ANN controller

Items	GP-SF-SS scheme A	GP-SF-SS scheme B	GP-SF-SS scheme C	GP-SF-SS scheme D	GP-SF-SS scheme E	GP-SF-SS scheme F	GP-SF-SS scheme G	GP-SF-SS scheme H
RMS motor voltage (PU)	0.9520	0.9389	0.9414	0.9542	0.9485	0.9407	0.9524	0.9261
RMS motor current (PU)	0.7269	0.6943	0.7509	0.6576	0.7081	0.6807	0.7401	0.6853
Maximum Transient Voltage over/under shoot (PU)	0.0866	0.0951	0.0878	0.0862	0.0938	0.0916	0.0888	0.0898
Maximum transient Current over/under Shoot (PU)	0.0859	0.0955	0.0952	0.0886	0.0920	0.0875	0.0923	0.0894
System efficiency	0.9012	0.8527	0.8905	0.8908	0.8555	0.8942	0.8759	0.8630
NMSE_V $\times 10^{-1}$	0.3378	0.5472	0.5005	0.8032	0.5105	0.5542	0.2851	0.6072
NMSE_ω_m $\times 10^{-1}$	0.6218	0.6720	0.6079	0.7635	0.2514	0.8283	0.9618	0.6750
NMSE_I $\times 10^{-1}$	0.2170	0.6127	0.2366	0.9221	0.7448	0.8563	0.2523	0.5160
THDv_bus L (%)	8.0866	8.8861	7.9180	7.1127	8.9779	7.0492	8.1413	8.9164
THDi_bus L (%)	8.8441	8.2750	8.4412	8.9262	7.9386	7.3801	8.2725	8.0730
THDv_bus M (%)	7.7610	8.5900	8.7014	7.6675	8.2304	8.6072	7.0900	8.7596
THDi_bus M (%)	8.4061	8.6479	8.8828	7.8089	7.9789	7.2004	8.8978	8.3977
Motor power factor	0.8909	0.8825	0.8938	0.8563	0.8718	0.8625	0.8862	0.8584
Reduction in KWh consumption (%)	12.6386	12.7662	12.0525	12.6566	13.8291	12.4920	13.1753	13.0346

Table 6: System dynamic behavior comparison using the FLC controller

Items	GP-SF-SS scheme A	GP-SF-SS scheme B	GP-SF-SS scheme C	GP-SF-SS scheme D	GP-SF-SS scheme E	GP-SF-SS scheme F	GP-SF-SS scheme G	GP-SF-SS scheme H
RMS motor voltage (PU)	0.9443	0.9517	0.9419	0.9525	0.9403	0.9593	0.9356	0.9493
RMS motor current (PU)	0.7443	0.7292	0.7331	0.7356	0.7204	0.6711	0.6787	0.7158
Maximum transient Voltage over/under shoot (PU)	0.0930	0.0952	0.0920	0.0965	0.0944	0.0875	0.0949	0.0879
Maximum transient current Over/under shoot (PU)	0.0928	0.0931	0.0942	0.0899	0.0906	0.0911	0.0924	0.0877
System efficiency	0.8788	0.8575	0.8534	0.8545	0.8616	0.8789	0.8863	0.8789
NMSE_V $\times 10^{-1}$	0.4076	0.3662	0.1461	0.4374	0.2244	0.2338	0.4377	0.6551
NMSE_ω_m $\times 10^{-1}$	0.7776	0.4769	0.2580	0.4247	0.9460	0.5037	0.8576	0.2416
NMSE_I $\times 10^{-1}$	0.4893	0.8974	0.9482	0.5073	0.4057	0.2905	0.3816	0.8778
THDv_bus L (%)	8.4756	9.8340	7.9340	7.6680	9.1958	6.4685	8.3135	6.8687
THDi_bus L (%)	7.5479	7.1746	8.4469	9.6391	6.0443	9.1476	8.6664	9.7769
THDv_bus M (%)	6.2888	6.1939	8.8543	9.1573	7.0203	8.7167	7.1567	6.3369
THDi_bus M (%)	9.3727	6.3183	8.8582	6.5006	7.7203	8.2898	8.4577	8.0611
Motor power factor	0.8837	0.8697	0.8903	0.8581	0.8795	0.9047	0.8685	0.8787
Reduction in KWh consumption (%)	13.2319	12.6070	13.7407	12.1542	13.9029	12.2293	13.2564	12.3885

assessment and prototyping, system parameters selection and optimization of control settings. The use of GA and PSO-search algorithm is used in online gain adjusting to minimize controller absolute value of total error. This is required before full scale prototyping which is both expensive and time consuming. The effectiveness of dynamic simulators brings on detailed sub-models selections and tested sub-models Matlab library of power system components already tested and validated. The dynamic simulation conditions are identical for all tuned controllers. To compare the global performances of all controllers, the Normalised Mean Square Error (NMSE) deviations between output plant variables and desired values and is defined as:

$$NMSE_{VS} = \frac{\sum (V_S - V_{S-ref})^2}{\sum (V_{S-ref})^2} \quad (29)$$

$$NMSE_{\omega m} = \frac{\sum (\omega_m - \omega_{m-ref})^2}{\sum (\omega_{m-ref})^2} \quad (30)$$

$$NMSE_{I_S} = \frac{\sum (I_S - I_{S-ref})^2}{\sum (I_{S-ref})^2} \quad (31)$$

The control system comprises the three dynamic multi-loop error driven regulator is co-ordinated to minimize the selected objective functions. SOO obtains a single global or near optimal solution based on a single weighted objective function. The weighted single objective function combines several objective functions using specified or selected weighting factors as follows:

$$= \alpha_1 J_1 + \alpha_2 J_2 + \alpha_3 J_3 + \alpha_4 J_4 + \alpha_5 J_5 \quad (32)$$

Where $\alpha_1 = 0.20$, $\alpha_2 = 0.20$, $\alpha_3 = 0.20$, $\alpha_4 = 0.20$, $\alpha_5 = 0.20$ are selected weighting factors. J_1, J_2, J_3, J_4 and J_5 are the selected objective functions. On the other hand, the MO finds the set of acceptable (trade-off) optimal solutions. This set of accepted solutions is called Pareto front. These acceptable trade-off multi level solutions give more ability to the user to make an informed decision by seeing a wide range of near optimal selected solutions.

Self tuned conventional PID controller: Table 7 shows the system behavior using traditional controllers with constant controller gains for the (GP-SF-SS) eight schemes. In addition, Table 8 shows system behavior comparison using the SOGA based Tuned conventional PID controller and Table 9 shows the system behavior comparison using the MOGA based Tuned conventional PID controller.

Finally, Table 10 and 11 show system behavior comparison using the SOPSO and MOPSO, respectively based tuned conventional PID controller. Comparing the system dynamic response results of the two study cases, with GA and PSO tuning algorithms and traditional controllers with constant controller gains results, ANN controller and FLC, it is quite apparent that the GA and PSO tuning algorithms highly improved the system dynamic performance from a general power quality point of view. The GA and PSO tuning algorithms had a great impact on Motor RMS voltage (PU) is improved from 0.8782 (without the (GP-SF-SS) device), 0.9500 (constant gains controller), 0.9414 (ANN controller) and 0.9525 (FLC) to around 0.9675 (SOGA based tuned controller), 0.9785 (MOGA based tuned controller), 0.9627 (SOPSO) based tuned controller and 0.9735 (MOPSO based tuned controller).

Motor RMS current (PU) is reduced from 0.8576 (without the (GP-SF-SS) device), 0.7064 (constant gains controller), 0.7269 (ANN controller) and 0.7158 (FLC) to around 0.6376 (SOGA based tuned controller), 0.6453 (MOGA based tuned controller), 0.6606 (SOPSO) based tuned controller and 0.5824 (MOPSO based tuned controller). Maximum Transient Motor Voltage Over/Under Shoot (PU) is reduced from 0.1597 (without the (GP-SF-SS) device), 0.0858 (constant gains controller), 0.0888 (ANN controller) and 0.0949 (FLC) to around 0.0240 (SOGA based tuned controller), 0.0469 (MOGA based tuned controller), 0.0321 (SOPSO) based tuned controller and 0.0483 (MOPSO based tuned controller).

Table 7: System dynamic behavior comparison using the constant parameters conventional PID controller

Items	GP-SF-SS scheme A	GP-SF-SS scheme B	GP-SF-SS scheme C	GP-SF-SS scheme D	GP-SF-SS scheme E	GP-SF-SS scheme F	GP-SF-SS scheme G	GP-SF-SS scheme H
RMS motor voltage (PU)	0.9500	0.9496	0.9586	0.9285	0.9462	0.9538	0.9256	0.9546
RMS motor current (PU)	0.7064	0.6562	0.6593	0.6785	0.6930	0.6998	0.7454	0.7126
Maximum transient voltage over/under shoot (PU)	0.0858	0.0944	0.0914	0.0881	0.0869	0.0875	0.0902	0.0902
Maximum transient current over/under shoot (PU)	0.0864	0.0961	0.0874	0.0900	0.0892	0.0876	0.0956	0.0893
System efficiency	0.8954	0.8677	0.8895	0.8980	0.8867	0.8976	0.9011	0.9017
NMSE_V $\times 10^{-1}$	0.1721	0.3234	0.1288	0.9623	0.1973	0.8957	0.2262	0.2868
NMSE_ω_m $\times 10^{-1}$	0.2519	0.7748	0.5897	0.6793	0.8571	0.6321	0.9128	0.3555
NMSE_I $\times 10^{-1}$	0.7644	0.2392	0.6403	0.6435	0.8015	0.3830	0.4092	0.3282
THDv_bus L (%)	6.8208	8.6008	6.9478	8.7799	7.5528	7.5302	7.5970	6.5950
THDi_bus L (%)	9.3836	6.1051	9.5581	8.4434	6.2780	8.4436	8.9070	8.9680
THDv_bus M (%)	9.1149	8.1016	7.8787	7.7108	8.4200	6.3196	8.1044	6.8222
THDi_bus M (%)	7.0554	7.1384	9.1692	7.5970	8.0389	9.5442	7.4731	8.4674
Motor power factor	0.8872	0.8836	0.8733	0.8590	0.8679	0.8763	0.8786	0.8924
Reduction in KWh consumption (%)	13.6978	12.7728	12.2793	12.3231	13.2706	13.8245	13.9720	12.2578

Table 8: System dynamic behavior comparison using the SOGA based tuned conventional PID controller

Items	GP-SF-SS scheme A	GP-SF-SS scheme B	GP-SF-SS scheme C	GP-SF-SS scheme D	GP-SF-SS scheme E	GP-SF-SS scheme F	GP-SF-SS scheme G	GP-SF-SS scheme H
RMS motor voltage (PU)	0.9675	0.9698	0.9697	0.9842	0.9723	0.9697	0.9630	0.9894
RMS motor current (PU)	0.6376	0.6007	0.6413	0.6399	0.5921	0.5820	0.6036	0.5905
Maximum transient voltage over/under shoot (PU)	0.0240	0.0419	0.0431	0.0402	0.0444	0.0323	0.0304	0.0322
Maximum transient current over/under shoot (PU)	0.0415	0.0265	0.0445	0.0348	0.0419	0.0495	0.0319	0.0422
System efficiency	0.9167	0.9350	0.9163	0.9413	0.9128	0.9461	0.9327	0.9292
NMSE_V $\times 10^{-2}$	0.8980	0.7120	0.7143	0.2404	0.7122	0.1748	0.1567	0.5586
NMSE_ω_m $\times 10^{-2}$	0.6660	0.3110	0.2314	0.3145	0.8576	0.8462	0.6678	0.8576
NMSE_I $\times 10^{-2}$	0.9340	0.9194	0.8680	0.5706	0.8056	0.3187	0.4223	0.6899
THDv_bus L (%)	3.6738	4.7325	3.1557	5.1047	4.4011	5.8094	5.7888	3.4243
THDi_bus L (%)	3.3040	5.0623	5.4013	5.3442	4.5590	4.0523	4.4384	3.9562
THDv_bus M (%)	5.5256	3.2876	5.7117	4.7700	5.1726	4.7771	4.6598	3.8161
THDi_bus M (%)	5.1057	4.4888	5.5620	5.0211	4.1383	4.8379	3.8825	3.2618
Motor power factor	0.9444	0.9193	0.9231	0.9644	0.9294	0.9345	0.9196	0.9408
Reduction in KWh consumption (%)	16.9568	16.9499	16.9364	16.8586	17.8487	16.0359	16.6263	16.1241

Table 9: System dynamic behavior comparison using a selected solution from the MOGA Pareto front based tuned conventional PID controller

Items	GP-SF-SS scheme A	GP-SF-SS scheme B	GP-SF-SS scheme C	GP-SF-SS scheme D	GP-SF-SS scheme E	GP-SF-SS scheme F	GP-SF-SS scheme G	GP-SF-SS scheme H
RMS motor voltage (PU)	0.9785	0.9960	0.9793	0.9776	0.9930	0.9814	0.9698	0.9867
RMS motor current (PU)	0.6453	0.6159	0.6123	0.6057	0.6582	0.6364	0.6017	0.6680
Maximum transient voltage over/under shoot (PU)	0.0469	0.0266	0.0231	0.0352	0.0245	0.0399	0.0483	0.0346
Maximum transient current over/under shoot (PU)	0.0368	0.0237	0.0356	0.0335	0.0300	0.0299	0.0428	0.0246
System efficiency	0.9581	0.9580	0.9400	0.9628	0.9432	0.9131	0.9215	0.9367
NMSE_V $\times 10^{-2}$	0.2800	0.2778	0.5814	0.1275	0.2492	0.5684	0.4771	0.4592
NMSE_ω_m $\times 10^{-2}$	0.8219	0.2763	0.6919	0.8953	0.1513	0.8633	0.4722	0.5006
NMSE_I $\times 10^{-2}$	0.6386	0.7455	0.9615	0.9035	0.1282	0.4371	0.6723	0.1359
THDv_bus L (%)	4.1615	3.4530	5.2564	3.5833	4.4201	3.8794	3.4402	5.7479
THDi_bus L (%)	3.6622	3.4313	3.2843	5.0090	4.9482	4.3160	4.5272	3.8655
THDv_bus M (%)	4.2924	5.7835	5.7618	4.8466	3.2841	5.2050	4.1642	3.8128
THDi_bus M (%)	3.4825	4.9829	4.4900	5.2857	5.2231	5.6462	5.0755	3.2916
Motor power factor	0.9425	0.9482	0.9287	0.9390	0.9355	0.9395	0.9313	0.9465
Reduction in KWh consumption (%)	16.7249	16.3605	16.3394	16.4113	16.8793	17.7564	17.0165	17.6754

Table 10: System dynamic behavior comparison using the SOPSO based tuned conventional PID controller

Items	GP-SF-SS scheme A	GP-SF-SS scheme B	GP-SF-SS scheme C	GP-SF-SS scheme D	GP-SF-SS scheme E	GP-SF-SS scheme F	GP-SF-SS scheme G	GP-SF-SS scheme H
RMS motor voltage (PU)	0.9627	0.9632	0.9570	0.9762	0.9624	0.9606	0.9680	0.9679
RMS motor current (PU)	0.6606	0.6648	0.6102	0.6194	0.6224	0.5934	0.5922	0.6279
Maximum transient voltage over/under shoot (PU)	0.0321	0.0310	0.0434	0.0301	0.0268	0.0411	0.0292	0.0346
Maximum transient current over/under shoot (PU)	0.0453	0.0464	0.0413	0.0429	0.0490	0.0330	0.0255	0.0420
System efficiency	0.9132	0.9571	0.9253	0.9328	0.9484	0.9581	0.9480	0.9193
NMSE_V $\times 10^{-2}$	0.6336	0.5588	0.6433	0.2308	0.4968	0.4609	0.8873	0.4541
NMSE_ω_m $\times 10^{-2}$	0.2746	0.8085	0.4723	0.4410	0.7228	0.6282	0.1817	0.2231
NMSE_I $\times 10^{-2}$	0.4257	0.5897	0.7433	0.9500	0.5263	0.1122	0.7787	0.4080
THDv_bus L (%)	4.0891	5.3808	4.9636	4.5919	3.2655	4.5906	4.9431	4.2308
THDi_bus L (%)	4.8129	3.1381	3.0904	5.0628	5.5267	5.6720	5.6368	5.1606
THDv_bus M (%)	5.7222	4.0662	3.2181	5.4751	3.8551	4.5867	5.2337	3.2203
THDi_bus M (%)	4.2410	5.4517	4.3424	3.8313	3.2064	4.8798	4.8041	5.0905
Motor power factor	0.9225	0.9638	0.9449	0.9148	0.9194	0.9335	0.9532	0.9205
Reduction in KWh consumption (%)	17.7855	16.0447	16.3018	17.6811	16.8949	17.8259	17.5114	17.4152

Table 11: System dynamic behavior comparison using a selected solution from the MOPSO Pareto front based yuned conventional PID controller

Items	GP-SF-SS scheme A	GP-SF-SS scheme B	GP-SF-SS scheme C	GP-SF-SS scheme D	GP-SF-SS scheme E	GP-SF-SS scheme F	GP-SF-SS scheme G	GP-SF-SS scheme H
RMS Motor voltage (PU)	0.9735	0.9693	0.9695	0.9871	0.9734	0.9820	0.9679	0.9876
RMS motor current (PU)	0.5824	0.6268	0.5973	0.6444	0.6026	0.6640	0.5923	0.6269
Maximum transient Voltage over/under Shoot (PU)	0.0483	0.0291	0.0362	0.0396	0.0330	0.0354	0.0427	0.0254
Maximum transient current Over/under shoot (PU)	0.0231	0.0322	0.0411	0.0479	0.0351	0.0254	0.0353	0.0482
System efficiency	0.9449	0.9642	0.9457	0.9242	0.9535	0.9120	0.9542	0.9229
NMSE_V $\times 10^{-2}$	0.3643	0.8212	0.1954	0.4308	0.6581	0.1409	0.3843	0.9323
NMSE_ω_m $\times 10^{-2}$	0.6804	0.1856	0.3299	0.2336	0.3484	0.7742	0.7158	0.6262
NMSE_I $\times 10^{-2}$	0.1455	0.8333	0.3079	0.5342	0.1375	0.6646	0.4535	0.7666
THDv_bus L (%)	3.8768	4.8055	4.5045	3.8953	4.3314	3.3968	5.1739	3.4034
THDi_bus L (%)	3.7437	4.4955	3.9741	4.8774	4.1384	3.3065	4.3281	4.5951
THDv_bus M (%)	4.2724	3.9660	3.7755	5.1568	4.1991	5.7096	5.3875	5.5552
THDi_bus M (%)	3.4044	3.0848	5.4816	4.7585	3.9809	4.9608	3.6366	3.6763
Motor power factor	0.9544	0.9203	0.9203	0.9206	0.9604	0.9530	0.9347	0.9256
Reduction in KWh consumption (%)	17.9147	16.5596	16.3489	17.7905	16.5059	17.3312	17.9808	17.3699

Maximum Transient Motor Current-Over/Under Shoot (PU) is reduced from 0.1775 (without the GP-SF-SS device), 0.0864 (constant gains controller), 0.0859 (ANN controller) and 0.0928 (FLC) to around 0.0415 (SOGA based tuned controller), 0.0368 (MOGA based tuned controller), 0.0453 (SOPSO) based tuned controller and 0.0231 (MOPSO based tuned controller). The system efficiency is improved from 0.8145 (without the GP-SF-SS

device), 0.8954 (constant gains controller), 0.9012 (ANN controller) and 0.8788 (FLC) to around 0.9167 (SOGA based tuned controller), 0.9581 (MOGA based tuned controller), 0.9132 (SOPSO) based tuned controller and 0.9449 (MOPSO based tuned controller). Moreover, the Normalized Mean Square Error (NMSE-V) of the Motor voltage is reduced from 0.3293 (without the GP-SF-SS device), 0.01721 (constant gains controller), 0.03378 (ANN controller) and 0.04076 (FLC) to around 0.008980 (SOGA based tuned controller), 0.002800 (MOGA based tuned controller), 0.006336 (SOPSO) based tuned controller and 0.003643 (MOPSO based tuned controller). In addition the (NMSE-ω_m) of the SPIM motor is reduced from 0.5093 (without the GP-SF-SS device), 0.02519 (constant gains controller), 0.06218 (ANN controller) and 0.07776 (FLC) to around 0.006660 (SOGA based tuned controller), 0.008219 (MOGA based tuned controller), 0.002746 (SOPSO) based tuned controller and 0.006804 (MOPSO based tuned controller).

The (NMSE-I) of the Motor current is reduced from 0.2398 (without the GP-SF-SS device), 0.07644 (constant gains controller), 0.02170 (ANN controller) and 0.04893 (FLC) to around 0.009340 (SOGA based tuned controller), 0.006386 (MOGA based tuned controller), 0.004257 (SOPSO) based tuned controller and 0.1455 (MOPSO based tuned controller). Total Harmonic Distortion THD (%) of the supply voltage is reduced from 17.486 (without the GP-SF-SS device), 6.8208 (constant gains controller), 8.0866 (ANN controller) and 8.4756 (FLC) to around 3.6738 (SOGA based tuned controller), 4.1615 (MOGA based tuned controller), 4.0891 (SOPSO) based tuned controller and 3.8768 (MOPSO based tuned controller).

THD (%) of the supply current is reduced from 19.475 (without the GP-SF-SS device), 9.3836 (constant gains controller), 8.8441 (ANN controller) and 7.5479 (FLC) to around 3.3040 (SOGA based tuned controller), 3.6622 (MOGA based tuned controller), 4.8129 (SOPSO) based tuned controller and 3.7437 (MOPSO based tuned controller). THD (%) of the motor voltage is reduced from 16.456 (without the GP-SF-SS device), 9.1149 (constant gains controller), 7.7610 (ANN controller) and 6.2888 (FLC) to around 5.5256 (SOGA based tuned controller), 4.2924 (MOGA based tuned controller), 5.7222 (SOPSO) based tuned controller and 4.2724 (MOPSO based tuned controller).

THD (%) of the motor current is reduced from 18.465 (without the GP-SF-SS device), 7.0554 (constant gains controller), 8.4061 (ANN controller) and 9.3727 (FLC) to around 5.1057 (SOGA based tuned controller), 3.4825 (MOGA based tuned controller), 4.2410 (SOPSO) based tuned controller and 3.4044 (MOPSO based tuned controller). Motor power factor is improved from 0.7516 (without the GP-SF-SS device), 0.8872 (constant gains controller), 0.8909 (ANN controller) and 0.8837 (FLC) to around 0.9444 (SOGA based tuned controller), 0.9425 (MOGA based tuned controller), 0.9225 (SOPSO) based tuned controller and 0.9544 (MOPSO based tuned controller). Reduction in KWh Consumption (%) is reduced from 0.000 (without the (GP-SF-SS) device), 12.6978 (constant gains controller), 13.6386 (ANN controller) and 13.2319 (FLC) to around 16.4767 (SOGA based tuned controller), 16.3532 (MOGA based tuned controller), 16.4862 (SOPSO) based tuned controller and 17.8901 (MOPSO based tuned controller).

Self tuned modified PID controller-I: Table 12 shows the system behavior using traditional controllers with constant controller gains for the (GP-SF-SS) eight schemes. In addition, Table 13 shows system behavior comparison using the SOGA based tuned modified PID controller-I and Table 14 shows the system behavior comparison using the MOGA based tuned modified PID controller-I.

Finally, Tables 15 and 16 show system behavior comparison using the SOPSO and MOPSO, respectively based Tuned modified PID controller-I. Comparing the system dynamic response results of the two study cases, with GA and PSO tuning algorithms and traditional controllers with constant controller gains results, ANN controller and FLC, it is quite apparent that the GA and PSO tuning algorithms highly improved the system dynamic performance from a general power quality point of view.

The GA and PSO tuning algorithms had a great impact on Motor RMS voltage (PU) is improved from 0.8782 (without the GP-SF-SS device), 0.9448 (constant gains controller), 0.9414 (ANN controller) and 0.9525 (FLC) to around 0.9851 (SOGA based tuned controller), 0.9917 (MOGA based tuned controller), 0.9669 (SOPSO) based tuned controller and 0.9737 (MOPSO based tuned controller). Motor RMS current (PU) is reduced from 0.8576 (without the GP-SF-SS device), 0.6845 (constant gains controller), 0.7269 (ANN controller) and 0.7158 (FLC) to around 0.6406 (SOGA based tuned controller), 0.6239 (MOGA based tuned controller), 0.6566 (SOPSO) based tuned controller and 0.6479 (MOPSO based tuned controller).

Maximum transient motor voltage over/under shoot (PU) is reduced from 0.1597 without the (GP-SF-SS device), 0.0938 (constant gains controller), 0.0888 (ANN controller) and 0.0949 (FLC) to around 0.0469 (SOGA based tuned controller), 0.0427 (MOGA based tuned controller), 0.0448 (SOPSO) based tuned controller and 0.0463 (MOPSO based tuned controller). Maximum

Table 12: System dynamic behavior comparison using the constant parameters modified PID controller-I

Items	GP-SF-SS scheme A	GP-SF-SS scheme B	GP-SF-SS scheme C	GP-SF-SS scheme D	GP-SF-SS scheme E	GP-SF-SS scheme F	GP-SF-SS scheme G	GP-SF-SS scheme H
RMS motor voltage (PU)	0.9448	0.9353	0.9337	0.9352	0.9410	0.9468	0.9343	0.9495
RMS motor current (PU)	0.6845	0.7002	0.7127	0.6670	0.7371	0.7504	0.7125	0.6530
Maximum transient voltage over/under shoot (PU)	0.0938	0.0903	0.0902	0.0913	0.0876	0.0915	0.0928	0.0860
Maximum transient current over/under shoot (PU)	0.0949	0.0946	0.0934	0.0908	0.0867	0.0947	0.0879	0.0907
System efficiency	0.9020	0.8864	0.9021	0.8765	0.8663	0.8555	0.8618	0.8704
NMSE_V $\times 10^{-1}$	0.4393	0.8723	0.4597	0.4333	0.1873	0.9501	0.8982	0.5059
NMSE_ω_m $\times 10^{-1}$	0.5909	0.5328	0.9598	0.1338	0.3333	0.3910	0.2167	0.7482
NMSE_I $\times 10^{-1}$	0.6488	0.2796	0.5075	0.3387	0.1149	0.2106	0.5887	0.8731
THDv_bus L (%)	6.6869	9.0298	7.4214	8.9958	7.3315	8.9853	6.5877	6.5893
THDi_bus L (%)	8.4680	6.3793	9.5771	7.8789	6.6467	7.0796	6.5232	6.1107
THDv_bus M (%)	6.9072	9.2573	8.8022	8.6810	7.4883	7.8586	9.7237	9.0211
THDi_bus M (%)	7.5903	9.6865	6.7759	8.0481	7.9518	7.8722	7.4673	8.0112
Motor power factor	0.9004	0.8526	0.9043	0.8611	0.8733	0.8731	0.8936	0.8787
Reduction in KWh consumption (%)	13.0035	12.8073	12.9952	13.2836	13.7859	13.5407	12.7883	12.2191

Table 13: System dynamic behavior comparison using the SOGA based tuned modified PID controller-I

Items	GP-SF-SS scheme A	GP-SF-SS scheme B	GP-SF-SS scheme C	GP-SF-SS scheme D	GP-SF-SS scheme E	GP-SF-SS scheme F	GP-SF-SS scheme G	GP-SF-SS scheme H
RMS motor voltage (PU)	0.9851	0.9933	0.9714	0.9894	0.9537	0.9945	0.9587	0.9577
RMS motor current (PU)	0.6406	0.6662	0.5973	0.5900	0.6309	0.6672	0.5821	0.6583
Maximum transient voltage over/under shoot (PU)	0.0469	0.0270	0.0321	0.0474	0.0362	0.0244	0.0423	0.0220
Maximum transient current over/under shoot (PU)	0.0386	0.0485	0.0329	0.0422	0.0409	0.0491	0.0275	0.0384
System efficiency	0.9377	0.9301	0.9341	0.9182	0.9394	0.9635	0.9293	0.9299
NMSE_V $\times 10^{-2}$	0.8807	0.7089	0.3113	0.5636	0.7984	0.7089	0.1122	0.3551
NMSE_ω_m $\times 10^{-2}$	0.2576	0.2852	0.1926	0.1449	0.4474	0.3110	0.2079	0.4817
NMSE_I $\times 10^{-2}$	0.3525	0.8410	0.1416	0.9499	0.9267	0.9517	0.8104	0.1488
THDv_bus L (%)	5.1191	3.5982	3.6842	5.5626	5.2495	3.5393	4.4520	3.1943
THDi_bus L (%)	3.6054	5.6580	4.1341	3.1982	3.1457	3.0392	5.3325	5.6098
THDv_bus M (%)	4.3007	3.4859	4.3528	5.3505	5.4255	5.7485	5.3200	3.7695
THDi_bus M (%)	4.4072	3.4605	4.8632	5.0777	3.0322	5.5927	4.8935	3.1622
Motor power factor	0.9354	0.9250	0.9199	0.9228	0.9604	0.9428	0.9487	0.9573
Reduction in Kwh consumption (%)	16.6603	16.7632	16.8202	17.2214	16.2669	16.1018	16.9524	17.7845KWh

Table 14: System dynamic behavior comparison using a selected solution from the MOGA pareto front based tuned modified PID controller-I

Items	GP-SF-SS scheme A	GP-SF-SS scheme B	GP-SF-SS scheme C	GP-SF-SS scheme D	GP-SF-SS scheme E	GP-SF-SS scheme F	GP-SF-SS scheme G	GP-SF-SS scheme H
RMS motor voltage (PU)	0.9917	0.9875	0.9692	0.9654	0.9923	0.9711	0.9741	0.9852
RMS motor current (PU)	0.6239	0.6693	0.6136	0.6278	0.5963	0.6252	0.6180	0.6394
Maximum transient Voltage over/under shoot (PU)	0.0427	0.0323	0.0345	0.0229	0.0375	0.0322	0.0439	0.0440
Maximum transient current Over/under shoot (PU)	0.0325	0.0289	0.0314	0.0488	0.0352	0.0321	0.0431	0.0323
System efficiency	0.9325	0.9373	0.9441	0.9465	0.9524	0.9356	0.9460	0.9268
NMSE_V $\times 10^{-2}$	0.3610	0.7281	0.2009	0.9099	0.5032	0.9540	0.4650	0.8030
NMSE_ω_m $\times 10^{-2}$	0.1543	0.6375	0.4557	0.6252	0.3093	0.8199	0.1710	0.3102
NMSE_I $\times 10^{-2}$	0.5272	0.9220	0.1698	0.4907	0.2897	0.8010	0.5422	0.7674
THDv_bus L (%)	5.7369	4.2281	3.5144	4.1456	4.9191	4.3935	4.1038	4.6154
THDi_bus L (%)	5.3255	4.3269	5.5917	5.5565	3.6072	5.4936	3.6929	4.9569
THDv_bus M (%)	3.4279	5.2190	4.2872	3.4898	3.7474	5.0843	3.1952	3.3422
THDi_bus M (%)	5.1945	5.8020	3.6985	4.3412	3.1218	5.1064	5.4246	4.4830
Motor power factor	0.9350	0.9283	0.9556	0.9484	0.9400	0.9213	0.9595	0.9549
Reduction in KWh consumption (%)	17.3211	16.4108	17.7319	16.3764	16.3702	18.0362	16.9144	16.7126

transient motor current-over/under shoot (PU) is reduced from 0.1775 (without the (GP-SF-SS) device), 0.0949 (constant gains controller), 0.0859 (ANN controller) and 0.0928 (FLC) to around 0.0386 (SOGA based tuned controller), 0.0325 (MOGA based tuned controller), 0.0333 (SOPSO) based tuned controller and 0.0298 (MOPSO based tuned controller). The system efficiency is improved from 0.8145 (without the (GP-SF-SS) device), 0.9020 (constant gains controller), 0.9012 (ANN controller) and 0.8788 (FLC) to around 0.9377 (SOGA based tuned

Table 15: System dynamic behavior comparison using the SOPSO based tuned modified PID controller-I

Items	GP-SF-SS scheme A	GP-SF-SS scheme B	GP-SF-SS scheme C	GP-SF-SS scheme D	GP-SF-SS scheme E	GP-SF-SS scheme F	GP-SF-SS scheme G	GP-SF-SS scheme H
RMS motor voltage (PU)	0.9669	0.9564	0.9743	0.9834	0.9718	0.9773	0.9556	0.9642
RMS motor current (PU)	0.6566	0.6106	0.6220	0.6622	0.6006	0.6576	0.6391	0.6602
Maximum transient Voltage over/under shoot (PU)	0.0448	0.0256	0.0465	0.0362	0.0487	0.0252	0.0232	0.0324
Maximum transient current Over/under shoot (PU)	0.0333	0.0330	0.0336	0.0323	0.0471	0.0405	0.0486	0.0264
System efficiency	0.9274	0.9347	0.9491	0.9124	0.9244	0.9332	0.9165	0.9588
NMSE_V $\times 10^{-2}$	0.3016	0.7941	0.1445	0.7363	0.9266	0.3960	0.3912	0.5889
NMSE_ω_m $\times 10^{-2}$	0.7334	0.3718	0.8095	0.8041	0.5268	0.4805	0.2317	0.6028
NMSE_I $\times 10^{-2}$	0.2851	0.4681	0.2859	0.6967	0.8208	0.3545	0.4293	0.5868
THDv_bus L (%)	5.5613	4.9424	3.3938	4.3591	5.7576	4.4323	4.1447	5.8164
THDi_bus L (%)	5.5307	3.5468	3.7122	3.7200	3.5134	3.9672	4.1706	4.7858
THDv_bus M (%)	5.0449	5.4019	5.2373	5.8435	4.6793	4.0421	4.0792	5.8135
THDi_bus M (%)	4.1944	3.2169	5.5222	5.3746	3.9132	5.5614	5.1515	3.4532
Motor power factor	0.9616	0.9558	0.9146	0.9558	0.9325	0.9355	0.9123	0.9267
Reduction in KWh consumption (%)	17.7759	16.4947	17.6530	17.8624	16.4938	16.5088	16.1253	16.1832

Table 16: System dynamic behavior comparison using a selected solution from the MOPSO Pareto front based tuned modified PID controller-I

Items	GP-SF-SS scheme A	GP-SF-SS scheme B	GP-SF-SS scheme C	GP-SF-SS scheme D	GP-SF-SS scheme E	GP-SF-SS scheme F	GP-SF-SS scheme G	GP-SF-SS scheme H
RMS motor voltage (PU)	0.9737	0.9793	0.9670	0.9951	0.9828	0.9779	0.9807	0.9752
RMS motor current (PU)	0.6479	0.6397	0.6595	0.6045	0.6177	0.5992	0.5832	0.5873
Maximum transient voltage over/under shoot (PU)	0.0463	0.0397	0.0441	0.0340	0.0491	0.0245	0.0365	0.0370
Maximum transient current over/under shoot (PU)	0.0298	0.0322	0.0237	0.0370	0.0451	0.0259	0.0266	0.0238
System efficiency	0.9262	0.9615	0.9236	0.9219	0.9268	0.9477	0.9436	0.9325
NMSE_V $\times 10^{-2}$	0.4001	0.8822	0.3119	0.4564	0.3901	0.4490	0.3510	0.6597
NMSE_ω_m $\times 10^{-2}$	0.3602	0.9359	0.4579	0.2908	0.1323	0.7642	0.4883	0.1928
NMSE_I $\times 10^{-2}$	0.1147	0.2940	0.7839	0.8108	0.2384	0.6547	0.6095	0.2877
THDv_bus L (%)	3.0994	3.9875	5.7828	4.6533	5.2011	4.7932	5.0948	3.4442
THDi_bus L (%)	4.7972	4.5219	5.8193	3.8786	3.5328	4.6316	4.3412	4.1310
THDv_bus M (%)	4.3214	5.1195	4.9136	3.1056	4.0126	3.2539	3.1939	5.1713
THDi_bus M (%)	5.7553	4.4751	5.4657	3.6590	3.7103	5.5636	5.0273	5.7794
Motor power factor	0.9259	0.9521	0.9350	0.9388	0.9381	0.9169	0.9634	0.9344
Reduction in KWh consumption (%)	16.9925	17.1471	16.2695	16.9366	17.4730	17.8310	16.5771	16.5401

controller), 0.9325 (MOGA based tuned controller), 0.9274 (SOPSO) based tuned controller and 0.9262 (MOPSO based tuned controller). Moreover, the Normalized Mean Square Error (NMSE-V) of the Motor voltage is reduced from 0.3293 (without the (GP-SF-SS) device), 0.04393 (constant gains controller), 0.03378 (ANN controller) and 0.04076 (FLC) to around 0.008807 (SOGA based tuned controller), 0.003610 (MOGA based tuned controller), 0.003016 (SOPSO) based tuned controller and 0.004001 (MOPSO based tuned controller).

In addition the (NMSE-ω_m) of the SPIM motor is reduced from 0.5093 (without the (GP-SF-SS) device), 0.05909 (constant gains controller), 0.06218 (ANN controller) and 0.07776 (FLC) to around 0.002576 (SOGA based tuned controller), 0.001543 (MOGA based tuned controller), 0.007334 (SOPSO) based tuned controller and 0.003602 (MOPSO based tuned controller). The (NMSE-I) of the Motor current is reduced from 0.2398 (without the GP-SF-SS device), 0.06488 (constant gains controller), 0.02170 (ANN controller) and 0.04893 (FLC) to around 0.003525 (SOGA based tuned controller), 0.005272 (MOGA based tuned controller), 0.002851 (SOPSO) based tuned controller and 0.001147 (MOPSO based tuned controller). Total Harmonic Distortion THD (%) of the supply voltage is reduced from 17.486 (without the (GP-SF-SS) device), 6.6869 (constant gains controller), 8.0866 (ANN controller) and 8.4756 (FLC) to around 5.1191 (SOGA based tuned controller), 5.7369 (MOGA based tuned controller), 5.5613 (SOPSO) based tuned controller and 3.0994 (MOPSO based tuned controller).

THD (%) of the supply current is reduced from 19.475 (without the GP-SF-SS device), 8.4680 (constant gains controller), 8.8441 (ANN controller) and 7.5479 (FLC) to around 3.6054 (SOGA based tuned controller), 5.3255 (MOGA based tuned controller), 5.5307 (SOPSO) based tuned controller and 4.7972 (MOPSO based tuned controller). THD (%) of the motor voltage is reduced from 16.456 (without the GP-SF-SS device), 6.9072 (constant gains controller), 7.7610 (ANN controller) and 6.2888 (FLC) to around 4.3007 (SOGA based tuned controller),

3.4279 (MOGA based tuned controller), 5.0449 (SOPSO) based tuned controller and 4.3214 (MOPSO based tuned controller). THD (%) of the motor current is reduced from 18.465 (without the GP-SF-SS device), 7.5903 (constant gains controller), 8.4061 (ANN controller) and 9.3727 (FLC) to around 4.4072 (SOGA based tuned controller), 5.1945 (MOGA based tuned controller), 4.1944 (SOPSO) based tuned controller and 5.7553 (MOPSO based tuned controller).

Motor power factor is improved from 0.7516 (without the GP-SF-SS device), 0.9004 (constant gains controller), 0.8909 (ANN controller) and 0.8837 (FLC) to around 0.9354 (SOGA based tuned controller), 0.9350 (MOGA based tuned controller), 0.9616 (SOPSO) based tuned controller and 0.9259 (MOPSO based tuned controller). Reduction in KWh Consumption (%) is reduced from 0.000 (without the GP-SF-SS device), 13.0035 (constant gains controller), 14.6386 (ANN controller) and 14.2319 (FLC) to around 17.8021 (SOGA based tuned controller), 17.9411 (MOGA based tuned controller), 17.3185 (SOPSO) based tuned controller and 17.7769 (MOPSO based tuned controller).

Self tuned modified PID controller- II: Table 17 shows the system behavior using traditional controllers with constant controller gains for the (GP-SF-SS) eight schemes. In addition, Table 18 shows system behavior comparison using the SOGA based Tuned modified PID controller-II and Table 19 shows the system behavior comparison using the MOGA based Tuned modified PID controller-II. Finally, Table 20 and 21 show system behavior comparison using the SOPSO and MOPSO respectively based tuned modified PID controller-II. Comparing the system dynamic response results of the two study cases with GA and PSO tuning algorithms and traditional controllers with constant controller gains results, ANN controller and FLC, it is quite apparent that the GA and PSO tuning algorithms highly improved the system dynamic performance from a general power quality point of view.

The GA and PSO tuning algorithms had a great impact on Motor RMS voltage (PU) is improved from 0.8782 (without the (GP-SF-SS) device), 0.9494 (constant gains controller), 0.9414 (ANN controller) and 0.9525 (FLC) to around 0.9728 (SOGA based tuned controller), 0.9877 (MOGA based tuned controller), 0.9691 (SOPSO) based tuned controller and 0.9658 (MOPSO based tuned controller). Motor RMS current (PU) is reduced from 0.8576 (without the GP-SF-SS device), 0.7353 (constant gains controller), 0.7269 (ANN controller) and 0.7158 (FLC) to around 0.5902 (SOGA based tuned controller), 0.6494 (MOGA based tuned controller), 0.6212 (SOPSO) based tuned controller and 0.6077 (MOPSO based tuned controller).

Maximum Transient Motor Voltage Over/Under Shoot (PU) is reduced from 0.1597 (without the GP-SF-SS device), 0.0859 (constant gains controller), 0.0888 (ANN controller) and 0.0949 (FLC) to around 0.0274 (SOGA based tuned controller), 0.0453 (MOGA based tuned controller), 0.0464 (SOPSO) based tuned controller and 0.0356 (MOPSO based tuned controller). Maximum Transient Motor Current-Over/Under Shoot (PU) is reduced from 0.1775 (without the GP-SF-SS device), 0.0925 (constant gains controller), 0.0859 (ANN controller) and 0.0928 (FLC) to around 0.0245 (SOGA based tuned controller), 0.0334 (MOGA based tuned controller), 0.0488 (SOPSO) based tuned controller and 0.0453 (MOPSO based tuned controller). The system efficiency is improved from 0.8145 (without the GP-SF-SS device), 0.8817 (constant gains controller), 0.9012 (ANN controller) and 0.8788 (FLC) to around

Table 17: System dynamic behavior comparison using the constant parameters modified PID controller-II

Items	GP-SF-SS scheme A	GP-SF-SS scheme B	GP-SF-SS scheme C	GP-SF-SS scheme D	GP-SF-SS scheme E	GP-SF-SS scheme F	GP-SF-SS scheme G	GP-SF-SS scheme H
RMS motor voltage (PU)	0.9494	0.9482	0.9542	0.9452	0.9531	0.9552	0.9554	0.9533
RMS motor current (PU)	0.7353	0.7141	0.7237	0.6597	0.6946	0.6894	0.6674	0.7375
Maximum transient Voltage over/under shoot (PU)	0.0859	0.0892	0.0953	0.0949	0.0894	0.0954	0.0910	0.0919
Maximum transient current Over/under shoot (PU)	0.0925	0.0930	0.0925	0.0933	0.0914	0.0936	0.0914	0.0924
System efficiency	0.8817	0.8891	0.8670	0.9043	0.8638	0.8785	0.8747	0.8793
NMSE_V $\times 10^{-1}$	0.7137	0.9628	0.8147	0.7674	0.4440	0.1155	0.4782	0.3914
NMSE_ω_m $\times 10^{-1}$	0.7818	0.4832	0.7179	0.9230	0.7152	0.2297	0.3882	0.7849
NMSE_I $\times 10^{-1}$	0.3573	0.7925	0.2951	0.4407	0.9076	0.9509	0.7527	0.6405
THDv_bus L (%)	9.1445	6.8204	7.5101	6.1985	7.1886	9.1371	8.6328	9.3997
THDi_bus L (%)	6.3350	7.9160	7.6691	7.3442	9.5192	6.6350	7.5065	9.7242
THDv_bus M (%)	6.2773	7.2342	6.5069	6.4651	6.6510	6.3815	8.0588	8.9402
THDi_bus M (%)	7.6200	9.2201	9.1022	6.0570	8.4897	6.4519	6.8475	9.5024
Motor power factor	0.8543	0.9031	0.8554	0.8789	0.8893	0.8850	0.8639	0.8854
Reduction in KWh consumption (%)	12.6287	13.8898	13.7387	12.9955	12.6808	13.3602	13.9421	13.9100

Table 18: System dynamic behavior comparison using the SOGA based tuned modified PID controller-II

Items	GP-SF-SS scheme A	GP-SF-SS scheme B	GP-SF-SS scheme C	GP-SF-SS scheme D	GP-SF-SS scheme E	GP-SF-SS scheme F	GP-SF-SS scheme G	GP-SF-SS scheme H
RMS motor voltage (PU)	0.9728	0.9752	0.9637	0.9811	0.9680	0.9939	0.9844	0.9717
RMS motor current (PU)	0.5902	0.6531	0.6617	0.5941	0.5910	0.6486	0.6450	0.6386
Maximum transient voltage over/under shoot (PU)	0.0274	0.0243	0.0478	0.0291	0.0275	0.0232	0.0387	0.0371
Maximum transient current over/under shoot (PU)	0.0245	0.0396	0.0342	0.0237	0.0323	0.0288	0.0476	0.0394
System efficiency	0.9280	0.9420	0.9233	0.9190	0.9638	0.9232	0.9191	0.9147
NMSE_V $\times 10^{-2}$	0.1593	0.4007	0.3164	0.5676	0.6894	0.2995	0.6774	0.2137
NMSE_ω_m $\times 10^{-2}$	0.8402	0.2551	0.6361	0.6549	0.7682	0.5775	0.4595	0.2931
NMSE_I $\times 10^{-2}$	0.6472	0.8215	0.7625	0.7631	0.7102	0.8097	0.2721	0.2798
THDv_bus L (%)	3.5030	3.7920	5.3193	4.1622	4.8884	3.8308	5.7405	4.6522
THDi_bus L (%)	3.7712	4.7880	4.9456	5.1057	5.6602	4.7600	5.1096	4.8218
THDv_bus M (%)	5.7026	4.5343	5.5958	3.8965	5.0717	4.1062	5.5637	3.2154
THDi_bus M (%)	5.1524	5.7183	4.1171	3.1807	4.0832	4.8812	5.0063	3.2784
Motor power factor	0.9538	0.9596	0.9120	0.9393	0.9450	0.9259	0.9330	0.9638
Reduction in KWh consumption (%)	16.1947	16.9438	16.9185	16.7393	16.3354	17.3915	17.4392	17.4965

Table 19: System dynamic behavior comparison using a selected solution from the MOGA Pareto front based tuned modified PID controller-II

Items	GP-SF-SS scheme A	GP-SF-SS scheme B	GP-SF-SS scheme C	GP-SF-SS scheme D	GP-SF-SS scheme E	GP-SF-SS scheme F	GP-SF-SS scheme G	GP-SF-SS scheme H
RMS motor voltage (PU)	0.9877	0.9732	0.9784	0.9935	0.9858	0.9715	0.9906	0.9842
RMS motor current (PU)	0.6494	0.6083	0.6374	0.6688	0.6253	0.6653	0.6545	0.6626
Maximum transient voltage over/under shoot (PU)	0.0453	0.0443	0.0457	0.0388	0.0376	0.0389	0.0247	0.0263
Maximum transient current over/under shoot (PU)	0.0334	0.0374	0.0293	0.0437	0.0326	0.0227	0.0381	0.0374
System efficiency	0.9451	0.9231	0.9605	0.9190	0.9633	0.9448	0.9459	0.9126
NMSE_V $\times 10^{-2}$	0.2924	0.7655	0.8916	0.3088	0.4079	0.7081	0.1263	0.5883
NMSE_ω_m $\times 10^{-2}$	0.6290	0.4958	0.1378	0.9557	0.1469	0.1525	0.2091	0.3759
NMSE_I$\times 10^{-2}$	0.7173	0.2170	0.5490	0.1939	0.7036	0.3465	0.5061	0.6605
THDv_bus L (%)	3.7913	3.7029	4.2263	4.7116	4.2097	5.1923	3.0945	4.9809
THDi_bus L (%)	4.2106	5.5442	3.9993	5.3079	5.8335	5.2306	5.4306	4.8899
THDv_bus M (%)	4.9854	4.7610	4.7671	5.3682	5.7911	4.2588	5.4148	4.1447
THDi_bus M (%)	4.5770	3.1418	3.6778	4.1496	3.3631	4.2735	3.1674	5.8402
Motor power factor	0.9456	0.9393	0.9395	0.9451	0.9623	0.9237	0.9647	0.9585
Reduction in KWh consumption (%)	16.0577	16.4092	17.2120	16.1411	16.7683	17.3021	17.4765	17.4260

Table 20: System dynamic behavior comparison using the SOPSO based tuned modified PID controller-II

Items	GP-SF-SS scheme A	GP-SF-SS scheme B	GP-SF-SS scheme C	GP-SF-SS scheme D	GP-SF-SS scheme E	GP-SF-SS scheme F	GP-SF-SS scheme G	GP-SF-SS scheme H
RMS motor voltage (PU)	0.9691	0.9713	0.9835	0.9842	0.9763	0.9825	0.9788	0.9663
RMS motor current (PU)	0.6212	0.6433	0.6324	0.6258	0.5867	0.5974	0.6142	0.6049
Maximum transient voltage over/under shoot (PU)	0.0464	0.0346	0.0441	0.0256	0.0237	0.0323	0.0322	0.0353
Maximum transient current over/under shoot (PU)	0.0488	0.0314	0.0289	0.0381	0.0364	0.0264	0.0354	0.0357
System efficiency	0.9210	0.9353	0.9518	0.9445	0.9254	0.9305	0.9444	0.9298
NMSE_V $\times 10^{-2}$	0.1438	0.8751	0.9360	0.2779	0.2432	0.2977	0.5851	0.8705
NMSE_ω_m $\times 10^{-2}$	0.3834	0.4972	0.4976	0.6141	0.7204	0.7205	0.3294	0.2099
NMSE_I $\times 10^{-2}$	0.2045	0.2107	0.4115	0.7322	0.4376	0.7131	0.4177	0.1244
THDv_bus L (%)	4.4817	5.7854	3.7209	4.9114	3.4368	4.1675	3.4236	3.9953
THDi_bus L (%)	4.3172	3.7147	5.3702	3.8792	3.1158	5.8145	4.3786	4.7285
THDv_bus M (%)	3.3625	4.4435	3.8304	3.3385	4.4359	4.0905	3.7869	5.7272
THDi_bus M (%)	4.7629	4.3552	4.4650	3.9976	3.2615	3.7452	4.5081	3.4193
Motor power factor	0.9202	0.9640	0.9277	0.9201	0.9616	0.9476	0.9346	0.9561
Reduction in KWh consumption (%)	16.0506	16.8014	17.4067	16.2125	16.0961	17.2636	17.2558	16.0565

0.9280 (SOGA based tuned controller), 0.9451 (MOGA based tuned controller), 0.9210 (SOPSO) based tuned controller and 0.9388 (MOPSO based tuned controller). Moreover, the Normalized Mean Square Error (NMSE-V) of the Motor voltage is reduced from 0.3293 (without the GP-SF-SS device), 0.07137 (constant gains controller), 0.03378 (ANN controller) and 0.04076 (FLC) to around 0.001593 (SOGA based tuned controller), 0.002924 (MOGA

Table 21: System dynamic behavior comparison using a selected solution from the MOPSO Pareto front based tuned modified PID controller-II

Items	GP-SF-SS scheme A	GP-SF-SS scheme B	GP-SF-SS scheme C	GP-SF-SS scheme D	GP-SF-SS scheme E	GP-SF-SS scheme F	GP-SF-SS scheme G	GP-SF-SS scheme H
RMS motor voltage (PU)	0.9658	0.9745	0.9654	0.9767	0.9858	0.9678	0.9661	0.9837
RMS motor current (PU)	0.6077	0.6634	0.6411	0.5867	0.5864	0.5811	0.6004	0.6265
Maximum transient voltage over/under shoot (PU)	0.0356	0.0229	0.0282	0.0310	0.0469	0.0306	0.0289	0.0339
Maximum transient current over/under shoot (PU)	0.0453	0.0270	0.0360	0.0344	0.0309	0.0324	0.0465	0.0430
System efficiency	0.9388	0.9367	0.9249	0.9419	0.9523	0.9302	0.9356	0.9393
NMSE_V $\times 10^{-2}$	0.2527	0.8499	0.5878	0.1414	0.2545	0.2573	0.1942	0.7567
NMSE_ω_m $\times 10^{-2}$	0.3195	0.7626	0.5715	0.9205	0.9568	0.1509	0.9511	0.3834
NMSE_I $\times 10^{-2}$	0.4985	0.7233	0.9082	0.5814	0.2122	0.5592	0.5918	0.2730
THDv_bus L (%)	4.5813	3.0403	3.3773	3.1796	5.1786	3.2238	5.0529	3.4189
THDi_bus L (%)	3.0598	3.0348	5.8151	5.3175	5.2004	5.5762	3.3719	3.2936
THDv_bus M (%)	5.5529	5.8125	5.6285	4.1372	4.8947	4.5492	3.6188	3.8853
THDi_bus M (%)	3.8990	3.9833	5.3316	3.0342	4.4183	4.7566	4.0797	3.5826
Motor power factor	0.9213	0.9406	0.9369	0.9508	0.9639	0.9473	0.9481	0.9583
Reduction in KWh consumption (%)	17.2531	17.2990	16.7742	17.1882	16.9379	16.1134	16.0796	16.6572

based tuned controller), 0.001438 (SOPSO) based tuned controller and 0.002527 (MOPSO based tuned controller). In addition the (NMSE-ω_m) of the SPIM motor is reduced from 0.5093 (without the GP-SF-SS device), 0.07818 (constant gains controller), 0.06218 (ANN controller) and 0.07776 (FLC) to around 0.008402 (SOGA based tuned controller), 0.006290 (MOGA based tuned controller), 0.003834 (SOPSO) based tuned controller and 0.003195 (MOPSO based tuned controller).

The (NMSE-I) of the motor current is reduced from 0.2398 (without the GP-SF-SS device), 0.03573 (constant gains controller), 0.02170 (ANN controller) and 0.04893 (FLC) to around 0.006472 (SOGA based tuned controller), 0.007173 (MOGA based tuned controller), 0.002045 (SOPSO) based tuned controller and 0.004985 (MOPSO based tuned controller).

Total Harmonic Distortion THD (%) of the supply voltage is reduced from 17.486 (without the GP-SF-SS device), 9.1445 (constant gains controller), 8.0866 (ANN controller) and 8.4756 (FLC) to around 3.5030 (SOGA based tuned controller), 3.7913 (MOGA based tuned controller), 4.4817 (SOPSO) based tuned controller and 4.5813 (MOPSO based tuned controller).

THD (%) of the supply current is reduced from 19.475 (without the GP-SF-SS device), 6.3350 (constant gains controller), 8.8441 (ANN controller) and 7.5479 (FLC) to around 3.7712 (SOGA based tuned controller), 4.2106 (MOGA based tuned controller), 4.3172 (SOPSO) based tuned controller and 3.0598 (MOPSO based tuned controller). THD (%) of the motor voltage is reduced from 16.456 (without the GP-SF-SS device), 6.2773 (constant gains controller), 7.7610 (ANN controller) and 6.2888 (FLC) to around 5.7026 (SOGA based tuned controller), 4.9854 (MOGA based tuned controller), 3.3625 (SOPSO) based tuned controller and 5.5529 (MOPSO based tuned controller).

THD (%) of the motor current is reduced from 18.465 (without the GP-SF-SS device), 7.6200 (constant gains controller), 8.4061 (ANN controller) and 9.3727 (FLC) to around 5.1524 (SOGA based tuned controller), 4.5770 (MOGA based tuned controller), 4.7629 (SOPSO) based tuned controller and 3.8990 (MOPSO based tuned controller). Motor power factor is improved from 0.7516 (without the GP-SF-SS device), 0.8543 (constant gains controller), 0.8909 (ANN controller) and 0.8837 (FLC) to around 0.9538 (SOGA based tuned controller), 0.9456 (MOGA based tuned controller), 0.9202 (SOPSO) based tuned controller and 0.9213 (MOPSO based tuned controller). Reduction in KWh Consumption (%) is reduced from 0.000 (without the GP-SF-SS device), 12.6287 (constant gains controller), 12.6386 (ANN controller) and 12.2319 (FLC) to around 16.5828 (SOGA based tuned controller), 17.1336 (MOGA based tuned controller), 16.0191 (SOPSO) based tuned controller and 17.4657 (MOPSO based tuned controller).

Self tuned Variable Structure Sliding Mode Controller (VSC/SMC/B-B): Table 22 shows the system behavior using traditional controllers with constant controller gains for the (GP-SF-SS) eight schemes.

Table 23 shows system behavior comparison using the SOGA based the self tuned variable structure sliding mode controller and Table 24 shows the system behavior comparison using the MOGA based the self tuned variable structure sliding mode controller.

Finally, Table 25 and 26 show system behavior comparison using the SOPSO and MOPSO, respectively based the self tuned variable structure sliding mode controller. Comparing the system dynamic response results of the two study cases, with GA and PSO tuning

Table 22: System dynamic behavior comparison using the constant parameters variable structure sliding mode controller

Items	GP-SF-SS scheme A	GP-SF-SS scheme B	GP-SF-SS scheme C	GP-SF-SS scheme D	GP-SF-SS scheme E	GP-SF-SS scheme F	GP-SF-SS scheme G	GP-SF-SS scheme H
RMS motor voltage (PU)	0.9433	0.9255	0.9255	0.9307	0.9426	0.9267	0.9360	0.9439
RMS motor current (PU)	0.7381	0.6974	0.7504	0.6655	0.7413	0.7308	0.6966	0.7152
Maximum transient voltage over/under shoot (PU)	0.0963	0.0948	0.0893	0.0922	0.0872	0.0886	0.0946	0.0931
Maximum transient current over/under shoot (PU)	0.0859	0.0919	0.0908	0.0957	0.0889	0.0865	0.0910	0.0965
System efficiency	0.8600	0.8684	0.8863	0.8962	0.8528	0.8733	0.8943	0.8603
NMSE_V $\times 10^{-1}$	0.3769	0.9310	0.9132	0.2972	0.7992	0.3404	0.8021	0.4641
NMSE_ω_m $\times 10^{-1}$	0.6436	0.5793	0.5509	0.1301	0.4771	0.1291	0.1325	0.5180
NMSE_I $\times 10^{-1}$	0.5613	0.9268	0.7721	0.2488	0.6421	0.7495	0.2426	0.6112
THDv_bus L (%)	6.5757	6.8160	9.2780	8.7515	6.3297	9.1557	7.3576	6.6441
THDi_bus L (%)	8.0879	9.5562	7.6951	8.0894	8.6950	6.0297	9.2242	9.4264
THDv_bus M (%)	6.0975	6.3986	7.4541	9.7252	8.3935	8.5866	7.7680	9.2297
THDi_bus M (%)	9.1725	8.0970	6.3755	7.1521	8.3271	6.7217	8.8283	8.1229
Motor power factor	0.8685	0.8854	0.8832	0.8548	0.8980	0.8905	0.8527	0.8914
Reduction in KWh consumption (%)	12.8652	12.9883	13.9106	13.5067	12.6772	12.7328	12.8655	13.5720

Table 23: System dynamic behavior comparison using the SOGA based tuned variable structure sliding mode controller

Items	GP-SF-SS scheme A	GP-SF-SS scheme B	GP-SF-SS scheme C	GP-SF-SS scheme D	GP-SF-SS scheme E	GP-SF-SS scheme F	GP-SF-SS scheme G	GP-SF-SS scheme H
RMS motor voltage (PU)	0.9897	0.9892	0.9767	0.9843	0.9841	0.9822	0.9781	0.9889
RMS motor current (PU)	0.6286	0.6361	0.6417	0.6410	0.6589	0.5812	0.6079	0.6501
Maximum transient voltage over/under shoot (PU)	0.0425	0.0400	0.0480	0.0450	0.0349	0.0394	0.0235	0.0369
Maximum transient current over/under shoot (PU)	0.0345	0.0459	0.0456	0.0350	0.0437	0.0401	0.0219	0.0255
System efficiency	0.9360	0.9250	0.9644	0.9418	0.9236	0.9585	0.9505	0.9572
NMSE_V $\times 10^{-2}$	0.9052	0.5126	0.7802	0.6428	0.1495	0.1789	0.5138	0.4751
NMSE_ω_m $\times 10^{-2}$	0.9566	0.5780	0.9161	0.2047	0.2551	0.4279	0.6962	0.9476
NMSE_I $\times 10^{-2}$	0.1561	0.1892	0.1810	0.6909	0.8941	0.1720	0.6173	0.3063
THDv_bus L (%)	5.3814	3.0527	3.1587	4.4393	3.8467	3.0609	5.2676	3.2121
THDi_bus L (%)	5.8074	4.0206	4.7807	4.4807	5.3266	4.4048	5.0903	5.0312
THDv_bus M (%)	4.5868	3.2134	4.4250	5.3862	4.3253	5.2276	4.4124	4.9892
THDi_bus M (%)	3.5953	3.7997	4.3836	4.1535	5.0078	3.9306	3.1589	5.2204
Motor power factor	0.9440	0.9549	0.9364	0.9168	0.9173	0.9583	0.9151	0.9569
Reduction in KWh consumption (%)	16.4575	17.3265	16.6721	17.9670	17.4947	16.8581	17.5310	16.5667

Table 24: System dynamic behavior comparison using a selected solution from the MOGA Pareto front based tuned variable structure sliding mode controller

Items	GP-SF-SS scheme A	GP-SF-SS scheme B	GP-SF-SS scheme C	GP-SF-SS scheme D	GP-SF-SS scheme E	GP-SF-SS scheme F	GP-SF-SS scheme G	GP-SF-SS scheme H
RMS motor voltage (PU)	0.9893	0.9899	0.9848	0.9864	0.9775	0.9842	0.9897	0.9933
RMS motor current (PU)	0.6394	0.5993	0.6342	0.6344	0.6394	0.5965	0.6373	0.5953
Maximum transient voltage over/under shoot (PU)	0.0401	0.0425	0.0315	0.0464	0.0315	0.0235	0.0418	0.0485
Maximum transient current over/under shoot (PU)	0.0262	0.0334	0.0245	0.0344	0.0460	0.0327	0.0289	0.0317
System efficiency	0.9429	0.9439	0.9378	0.9619	0.9303	0.9225	0.9171	0.9465
NMSE_V $\times 10^{-2}$	0.9433	0.4550	0.5516	0.5471	0.6182	0.4256	0.2076	0.6312
NMSE_ω_m $\times 10^{-2}$	0.5618	0.5446	0.2318	0.3872	0.5468	0.7479	0.7313	0.7201
NMSE_I $\times 10^{-2}$	0.4695	0.6063	0.3295	0.6326	0.6434	0.8820	0.6294	0.9610
THDv_bus L (%)	3.3714	5.5126	5.3215	5.1804	5.3135	4.9511	4.7887	4.0627
THDi_bus L (%)	5.1991	5.0793	5.6082	3.3219	5.5356	4.7045	3.0560	3.6958
THDv_bus M (%)	4.4394	4.2025	5.2826	5.5403	4.4735	4.1239	5.6535	3.8214
THDi_bus M (%)	5.2254	5.3110	5.0673	3.1500	4.7562	3.9698	4.6729	5.6042
Motor power factor	0.9623	0.9236	0.9438	0.9373	0.9591	0.9522	0.9357	0.9122
Reduction in KWh consumption (%)	17.7936	16.0550	17.5783	17.9888	18.0277	17.6206	16.9121	17.0328

algorithms and traditional controllers with constant controller gains results, ANN controller and FLC, it is quite apparent that the GA and PSO tuning algorithms highly improved the system dynamic performance from a general power quality point of view. The GA and PSO tuning algorithms had a great impact on Motor RMS voltage (PU) is improved from 0.8782 (without the GP-SF-SS device), 0.9433 (constant gains controller), 0.9414

Table 25: System dynamic behavior comparison using the SOPSO based tuned variable structure sliding mode controller

Items	GP-SF-SS scheme A	GP-SF-SS scheme B	GP-SF-SS scheme C	GP-SF-SS scheme D	GP-SF-SS scheme E	GP-SF-SS scheme F	GP-SF-SS scheme G	GP-SF-SS scheme H
RMS motor voltage (PU)	0.9806	0.9802	0.9927	0.9798	0.9915	0.9936	0.9798	0.9799
RMS motor current (PU)	0.5816	0.6537	0.6359	0.6304	0.6020	0.6540	0.6037	0.6478
Maximum transient voltage over/under shoot (PU)	0.0276	0.0263	0.0396	0.0219	0.0312	0.0295	0.0231	0.0245
Maximum transient Current over/under shoot (PU)	0.0333	0.0446	0.0461	0.0225	0.0421	0.0454	0.0421	0.0484
System efficiency	0.9567	0.9450	0.9449	0.9626	0.9275	0.9454	0.9401	0.9581
NMSE_V $\times 10^{-2}$	0.8955	0.1152	0.9075	0.3170	0.9514	0.7139	0.7336	0.8753
NMSE_ω_m $\times 10^{-2}$	0.4872	0.9507	0.7797	0.5850	0.2811	0.5647	0.1954	0.4885
NMSE_I $\times 10^{-2}$	0.3756	0.7838	0.7896	0.5872	0.7103	0.1617	0.3679	0.1525
THDv_bus L (%)	4.2650	3.4415	4.7792	5.1551	3.8153	4.5126	3.9054	3.5358
THDi_bus L (%)	5.5612	3.1049	3.8194	3.5532	4.7433	3.6139	5.8433	3.0693
THDv_bus M (%)	4.6731	4.9615	5.1879	5.5603	5.7558	5.5833	3.5268	5.7888
THDi_bus M (%)	3.7393	3.4340	3.9875	5.0950	3.1176	4.5609	4.6010	4.9156
Motor power factor	0.9444	0.9592	0.9498	0.9226	0.9176	0.9511	0.9523	0.9267
Reduction in KWh consumption (%)	16.9575	17.1734	17.6314	16.1444	17.2443	16.1263	16.8650	16.6417

Table 26: System dynamic behavior comparison using a selected solution from the MOPSO pareto front based tuned variable structure sliding mode controller

Items	GP-SF-SS scheme A	GP-SF-SS scheme B	GP-SF-SS scheme C	GP-SF-SS scheme D	GP-SF-SS scheme E	GP-SF-SS scheme F	GP-SF-SS scheme G	GP-SF-SS scheme H
RMS motor voltage (PU)	0.9760	0.9766	0.9881	0.9789	0.9923	0.9786	0.9785	0.9954
RMS motor current (PU)	0.6490	0.6400	0.5918	0.5886	0.5813	0.6059	0.6535	0.6687
Maximum transient voltage over/under shoot (PU)	0.0488	0.0354	0.0446	0.0397	0.0304	0.0402	0.0318	0.0480
Maximum transient current over/under shoot (PU)	0.0354	0.0244	0.0406	0.0362	0.0280	0.0420	0.0238	0.0487
System efficiency	0.9561	0.9371	0.9299	0.9407	0.9417	0.9610	0.9264	0.9276
NMSE_V $\times 10^{-2}$	0.8868	0.3567	0.8480	0.4443	0.4895	0.4691	0.9470	0.6252
NMSE_ω_m $\times 10^{-2}$	0.2801	0.6030	0.9367	0.6884	0.1285	0.4599	0.6357	0.3357
NMSE_I $\times 10^{-2}$	0.8297	0.3605	0.3022	0.3046	0.3535	0.8193	0.5832	0.5447
THDv_bus L (%)	3.8253	3.9468	4.3685	3.6609	5.7422	3.8885	5.2245	5.5537
THDi_bus L (%)	5.2151	4.2433	4.2551	3.6561	3.0591	4.0850	5.3932	3.8313
THDv_bus M (%)	4.2222	4.1980	4.1197	5.4412	5.3492	5.6062	5.3860	5.4766
THDi_bus M (%)	5.6939	3.0614	3.1751	5.1101	4.8191	5.6545	4.3254	4.4722
Motor power factor	0.9518	0.9198	0.9470	0.9244	0.9505	0.9256	0.9368	0.9574
Reduction in KWh consumption (%)	17.1977	17.5629	17.0965	17.3205	16.4476	16.7930	17.6094	17.4021

(ANN controller) and 0.9525 (FLC) to around 0.9897 (SOGA based tuned controller), 0.9893 (MOGA based tuned controller), 0.9806 (SOPSO) based tuned controller and 0.9760 (MOPSO based tuned controller). Motor RMS current (PU) is reduced from 0.8576 (without the GP-SF-SS device), 0.7381 (constant gains controller), 0.7269 (ANN controller) and 0.7158 (FLC) to around 0.6286 (SOGA based tuned controller), 0.6394 (MOGA based tuned controller), 0.5816 (SOPSO) based tuned controller and 0.6490 (MOPSO based tuned controller).

Maximum transient motor voltage over/Under shoot (PU) is reduced from 0.1597 (without the GP-SF-SS device), 0.0963 (constant gains controller), 0.0888 (ANN controller) and 0.0949 (FLC) to around 0.0425 (SOGA based tuned controller), 0.0401 (MOGA based tuned controller), 0.0276 (SOPSO) based tuned controller and 0.0488 (MOPSO based tuned controller). Maximum transient motor current-over/under shoot (PU) is reduced from 0.1775 (without the GP-SF-SS device), 0.0859 (constant gains controller), 0.0859 (ANN controller) and 0.0928 (FLC) to around 0.0345 (SOGA based tuned controller), 0.0262 (MOGA based tuned controller), 0.0333 (SOPSO) based tuned controller and 0.0354 (MOPSO based tuned controller). The system efficiency is improved from 0.8145 (without the GP-SF-SS device), 0.8600 (constant gains controller), 0.9012 (ANN controller) and 0.8788 (FLC) to around 0.9360 (SOGA based tuned controller), 0.9429 (MOGA based tuned controller), 0.9567 (SOPSO) based tuned controller and 0.9561 (MOPSO based tuned controller).

The Normalized Mean Square Error (NMSE-V) of the Motor voltage is reduced from 0.329 (without the GP-SF-SS device), 0.0376 (constant gains controller), 0.0337 (ANN controller) and 0.04076 (FLC) to around 0.0905 (SOGA based tuned controller), 0.00943 (MOGA based tuned controller), 0.008955 (SOPSO) based tuned controller and 0.008868 (MOPSO based tuned controller). In addition the (NMSE-ω_m) of the SPIM motor is reduced from 0.5093 (without the GP-SF-SS device), 0.06436 (constant gains controller), 0.06218 (ANN controller) and

Table 27: System dynamic behavior comparison using the constant parameters zonal activation or target practice controller

Items	GP-SF-SS scheme A	GP-SF-SS scheme B	GP-SF-SS scheme C	GP-SF-SS scheme D	GP-SF-SS scheme E	GP-SF-SS scheme F	GP-SF-SS scheme G	GP-SF-SS scheme H
RMS motor voltage (PU)	0.9382	0.9352	0.9344	0.9360	0.9368	0.9427	0.9286	0.9261
RMS motor current (PU)	0.7499	0.7172	0.6760	0.6870	0.6697	0.7015	0.6930	0.6987
Maximum transient voltage over/under shoot (PU)	0.0959	0.0919	0.0929	0.0942	0.0870	0.0858	0.0917	0.0859
Maximum transient Current over/under shoot (PU)	0.0907	0.0879	0.0944	0.0925	0.0860	0.0955	0.0941	0.0957
System efficiency	0.8673	0.8920	0.8574	0.8639	0.8778	0.8982	0.8826	0.8742
NMSE_V $\times 10^{-1}$	0.6263	0.6762	0.6123	0.8988	0.5377	0.8272	0.8963	0.6289
NMSE_ω_m $\times 10^{-1}$	0.8417	0.2866	0.5197	0.4371	0.4737	0.5362	0.1873	0.6084
NMSE_I $\times 10^{-1}$	0.1299	0.1159	0.5846	0.2074	0.7075	0.7526	0.3250	0.3244
THDv_bus L (%)	6.6196	9.5629	6.7957	6.0542	8.6596	7.5567	7.4748	9.4791
THDi_bus L (%)	9.6328	7.8362	6.0898	9.1605	6.2415	6.3669	8.6885	6.5851
THDv_bus M (%)	6.2423	6.2644	8.7887	6.1509	8.6849	6.8685	8.4157	7.9866
THDi_bus M (%)	8.2256	7.1214	9.4389	6.3763	7.1414	9.1679	9.8268	6.2814
Motor power factor	0.8950	0.8888	0.8753	0.8769	0.8987	0.8861	0.8596	0.8631
Reduction in KWh consumption (%)	12.8356	12.2520	13.3622	13.9313	13.2306	13.0419	12.7971	13.0469

0.07776 (FLC) to around 0.09566 (SOGA based tuned controller), 0.005618 (MOGA based tuned controller), 0.004872 (SOPSO) based tuned controller and 0.002801 (MOPSO based tuned controller).

The Normalized (NMSE-I) of the Motor current is reduced from 0.2398 (without the GP-SF-SS device), 0.05613 (constant gains controller), 0.02170 (ANN controller) and 0.04893 (FLC) to around 0.01561 (SOGA based tuned controller), 0.004695 (MOGA based tuned controller), 0.003756 (SOPSO) based tuned controller and 0.008297 (MOPSO based tuned controller). Total Harmonic Distortion THD (%) of the supply voltage is reduced from 17.486 (without the GP-SF-SS device), 6.5757 (constant gains controller), 8.0866 (ANN controller) and 8.4756 (FLC) to around 5.3814 (SOGA based tuned controller), 3.3714 (MOGA based tuned controller), 4.2650 (SOPSO) based tuned controller and 3.8253 (MOPSO based tuned controller).

THD (%) of the supply current is reduced from 19.475 (without the GP-SF-SS device), 8.0879 (constant gains controller), 8.8441 (ANN controller) and 7.5479 (FLC) to around 5.8074 (SOGA based tuned controller), 5.1991 (MOGA based tuned controller), 5.5612 (SOPSO) based tuned controller and 5.2151 (MOPSO based tuned controller).

THD (%) of the motor voltage is reduced from 16.456 (without the GP-SF-SS device), 6.0975 (constant gains controller), 7.7610 (ANN controller) and 6.2888 (FLC) to around 4.5868 (SOGA based tuned controller), 4.4394 (MOGA based tuned controller), 4.6731 (SOPSO based tuned controller) and 4.2222 (MOPSO based tuned controller). THD (%) of the motor current is reduced from 18.465 (without the GP-SF-SS device), 9.1725 (constant gains controller), 8.4061 (ANN controller) and 9.3727 (FLC) to around 3.5953 (SOGA based tuned controller), 5.2254 (MOGA based tuned controller), 3.7393 (SOPSO based tuned controller) and 5.6939 (MOPSO based tuned controller). Motor power factor is improved from 0.7516 (without the GP-SF-SS device), 0.8685 (constant gains controller), 0.8909 (ANN controller) and 0.8837 (FLC) to around 0.9440 (SOGA based tuned controller), 0.9623 (MOGA based tuned controller), 0.9444 (SOPSO based tuned controller) and 0.9518 (MOPSO based tuned controller). Reduction in KWh Consumption (%) is reduced from 0.000 (without the GP-SF-SS device), 12.8652 (constant gains controller), 12.6386 (ANN controller) and 12.2319 (FLC) to around 16.2051 (SOGA based tuned controller), 16.0151 (MOGA based tuned controller), 16.8778 (SOPSO) based tuned controller and 17.4786 (MOPSO based tuned controller).

Self tuned zonal activation or target practice controller: Table 27 shows the system behavior using traditional controllers with constant controller gains for the (GP-SF-SS) eight schemes. In addition, Table 28 shows system behavior comparison using the SOGA based the self tuned zonal activation or target practice controller and Table 29 shows the system behavior comparison using the MOGA based the self tuned zonal activation or target practice controller.

Finally, Table 30 and 31 show system behavior comparison using the SOPSO and MOPSO, respectively based the self tuned zonal activation or target practice controller.

Comparing the system dynamic response results of the two study cases, with GA and PSO tuning algorithms and traditional controllers with constant controller gains results, ANN controller and FLC, it is quite apparent that the GA and PSO tuning algorithms highly improved the system dynamic performance from a

Table 28: System dynamic behavior comparison using the SOGA based tuned zonal activation or target practice controller

Items	GP-SF-SS scheme A	GP-SF-SS scheme B	GP-SF-SS scheme C	GP-SF-SS scheme D	GP-SF-SS scheme E	GP-SF-SS scheme F	GP-SF-SS scheme G	GP-SF-SS scheme H
RMS motor voltage (PU)	0.9844	0.9928	0.9942	0.9804	0.9783	0.9929	0.9799	0.9882
RMS motor current (PU)	0.5857	0.6038	0.6700	0.5991	0.6249	0.6061	0.6405	0.6662
Maximum transient voltage over/under shoot (PU)	0.0432	0.0488	0.0417	0.0436	0.0285	0.0273	0.0292	0.0417
Maximum transient current over/under shoot (PU)	0.0490	0.0396	0.0370	0.0454	0.0442	0.0404	0.0405	0.0447
System efficiency	0.9255	0.9443	0.9356	0.9341	0.9337	0.9498	0.9173	0.9320
NMSE_V $\times 10^{-2}$	0.9344	0.4085	0.5162	0.8464	0.2071	0.4482	0.8398	0.7426
NMSE_ω_m $\times 10^{-2}$	0.7623	0.3127	0.7577	0.3099	0.5050	0.1420	0.5591	0.4524
NMSE_I $\times 10^{-2}$	0.8792	0.2581	0.1329	0.6171	0.5983	0.6088	0.4031	0.5892
THDv_bus L (%)	3.8914	4.3280	5.3682	3.8706	5.0285	3.2328	5.1433	4.3478
THDi_bus L (%)	5.2460	3.5087	3.6048	4.3353	3.2326	4.7089	3.5619	5.6653
THDv_bus M (%)	3.0758	4.4593	5.4804	5.2800	5.2819	3.5764	5.0420	3.6299
THDi_bus M (%)	4.7253	3.1828	3.2255	4.8194	5.5000	4.2307	5.0251	3.2203
Motor power factor	0.9378	0.9483	0.9311	0.9332	0.9392	0.9143	0.9645	0.9283
Reduction in KWh consumption (%)	16.1557	18.0242	17.2037	16.8814	17.0676	16.7003	16.9005	16.4818

Table 29: System dynamic behavior comparison using a selected solution from the MOGA Pareto front based tuned zonal activation or target practice controller

Items	GP-SF-SS scheme A	GP-SF-SS scheme B	GP-SF-SS scheme C	GP-SF-SS scheme D	GP-SF-SS scheme E	GP-SF-SS scheme F	GP-SF-SS scheme G	GP-SF-SS scheme H
RMS motor voltage (PU)	0.9948	0.9886	0.9928	0.9752	0.9778	0.9918	0.9838	0.9933
RMS motor current (PU)	0.6338	0.6654	0.6060	0.6600	0.5891	0.5859	0.6011	0.6640
Maximum transient voltage over/under shoot (PU)	0.0292	0.0270	0.0474	0.0253	0.0222	0.0321	0.0413	0.0466
Maximum transient current over/under shoot (PU)	0.0384	0.0262	0.0307	0.0283	0.0221	0.0329	0.0399	0.0242
System efficiency	0.9250	0.9612	0.9347	0.9145	0.9599	0.9638	0.9468	0.9505
NMSE_V $\times 10^{-2}$	0.4511	0.9186	0.8596	0.9551	0.4457	0.8968	0.5022	0.6763
NMSE_ω_m $\times 10^{-2}$	0.5567	0.9504	0.8794	0.6495	0.4077	0.3728	0.8807	0.2028
NMSE_I $\times 10^{-2}$	0.3647	0.8383	0.7341	0.6602	0.3407	0.7330	0.8730	0.5469
THDv_bus L (%)	4.5209	4.4647	3.6651	5.6658	4.4858	4.3206	5.2183	5.0969
THDi_bus L (%)	3.6205	5.4286	5.1228	4.1673	3.8845	4.3628	3.4311	4.4198
THDv_bus M (%)	5.4651	5.0247	5.8447	5.3287	5.2339	5.1812	5.5810	3.3135
THDi_bus M (%)	4.0933	5.1371	4.2741	3.3043	5.8288	4.5383	3.4023	3.3931
Motor power factor	0.9299	0.9129	0.9527	0.9362	0.9142	0.9171	0.9627	0.9442
Reduction in KWh consumption (%)	16.3008	16.0484	17.8331	16.4275	16.6290	17.3628	16.6000	16.9739

general power quality point of view. The GA and PSO tuning algorithms had a great impact on Motor RMS voltage (PU) is improved from 0.8782 (without the GP-SF-SS device), 0.9382 (constant gains controller), 0.9414 (ANN controller) and 0.9525 (FLC) to around 0.9844 (SOGA based tuned controller), 0.9948 (MOGA based tuned controller), 0.9901 (SOPSO) based tuned controller and 0.9851 (MOPSO based tuned controller).

Motor RMS current (PU) is reduced from 0.8576 (without the GP-SF-SS device), 0.7499 (constant gains controller), 0.7269 (ANN controller) and 0.7158 (FLC) to around 0.5857 (SOGA based tuned controller), 0.6338 (MOGA based tuned controller), 0.6310 (SOPSO) based tuned controller and 0.6306 (MOPSO based tuned controller). Maximum Transient Motor Voltage Over/Under Shoot (PU) is reduced from 0.1597 (without the GP-SF-SS device), 0.0959 (constant gains controller), 0.0888 (ANN controller) and 0.0949 (FLC) to around 0.0432 (SOGA based tuned controller), 0.0292 (MOGA based tuned controller), 0.0477 (SOPSO) based tuned controller and 0.0264 (MOPSO based tuned controller). Maximum Transient Motor Current-Over/Under Shoot (PU) is reduced from 0.1775 (without the GP-SF-SS device), 0.0907 (constant gains controller), 0.0859 (ANN controller) and 0.0928 (FLC) to around 0.0490 (SOGA based tuned controller), 0.0384 (MOGA based tuned controller), 0.0271 (SOPSO) based tuned controller and 0.0392 (MOPSO based tuned controller).

The system efficiency is improved from 0.8145 (without the GP-SF-SS device), 0.8673 (constant gains controller), 0.9012 (ANN controller) and 0.8788 (FLC) to around 0.9255 (SOGA based tuned controller), 0.9250 (MOGA based tuned controller), 0.9263 (SOPSO) based tuned controller and 0.9162 (MOPSO based tuned controller). Moreover, the Normalized Mean Square Error (NMSE-V) of the motor voltage is reduced from 0.3293

Table 30: System dynamic behavior comparison using the SOPSO based tuned zonal activation or target practice controller

Items	GP-SF-SS scheme A	GP-SF-SS scheme B	GP-SF-SS scheme C	GP-SF-SS scheme D	GP-SF-SS scheme E	GP-SF-SS scheme F	GP-SF-SS scheme G	GP-SF-SS scheme H
RMS motor voltage (PU)	0.9901	0.9891	0.9821	0.9784	0.9782	0.9789	0.9837	0.9925
RMS motor current (PU)	0.6310	0.5910	0.6270	0.5905	0.6493	0.6138	0.6541	0.5842
Maximum transient Voltage over/under shoot (PU)	0.0477	0.0327	0.0361	0.0244	0.0225	0.0263	0.0453	0.0463
Maximum transient current Over/under shoot (PU)	0.0271	0.0494	0.0417	0.0461	0.0352	0.0357	0.0299	0.0236
System efficiency	0.9263	0.9343	0.9490	0.9553	0.9557	0.9333	0.9465	0.9200
NMSE_V $\times 10^{-2}$	0.5837	0.8633	0.8423	0.6233	0.5233	0.1221	0.3497	0.6017
NMSE_ω_m $\times 10^{-2}$	0.8182	0.7129	0.4035	0.4548	0.5716	0.2737	0.4827	0.4605
NMSE_I $\times 10^{-2}$	0.2873	0.3622	0.3304	0.3785	0.5799	0.8206	0.3657	0.8602
THDv_bus L (%)	4.9241	3.9995	5.7948	4.0228	3.0770	5.3202	5.8011	3.9037
THDi_bus L (%)	5.8456	4.9748	5.7395	5.2148	3.0239	3.9422	4.5605	3.8886
THDv_bus M (%)	4.4285	3.3007	4.5897	4.2539	3.5344	3.4568	5.6623	3.4072
THDi_bus M (%)	5.1721	5.2724	3.9094	3.6887	4.4201	4.9596	5.6931	4.2641
Motor power factor	0.9174	0.9293	0.9257	0.9325	0.9595	0.9526	0.9248	0.9360
Reduction in KWh consumption (%)	17.0819	17.8053	16.3745	18.0068	16.5738	16.5351	17.7964	17.5163

Table 31: System dynamic behavior comparison using a selected solution from the MOPSO Pareto front based tuned zonal activation or target practice controller

Items	GP-SF-SS scheme A	GP-SF-SS scheme B	GP-SF-SS scheme C	GP-SF-SS scheme D	GP-SF-SS scheme E	GP-SF-SS scheme F	GP-SF-SS scheme G	GP-SF-SS scheme H
RMS motor voltage (PU)	0.9851	0.9917	0.9844	0.9844	0.9842	0.9835	0.9935	0.9751
RMS motor current (PU)	0.6306	0.6087	0.6137	0.6581	0.6135	0.5866	0.5980	0.5845
Maximum transient voltage over/under shoot (PU)	0.0264	0.0306	0.0227	0.0318	0.0226	0.0439	0.0496	0.0249
Maximum transient current over/under shoot (PU)	0.0392	0.0255	0.0305	0.0256	0.0281	0.0329	0.0256	0.0286
System efficiency	0.9162	0.9279	0.9214	0.9499	0.9538	0.9295	0.9534	0.9531
NMSE_V $\times 10^{-2}$	0.7559	0.3893	0.3321	0.7382	0.4850	0.3784	0.8828	0.7048
NMSE_ω_m $\times 10^{-2}$	0.7575	0.3393	0.6333	0.2588	0.2414	0.6953	0.2978	0.7634
NMSE_I $\times 10^{-2}$	0.1690	0.3168	0.4140	0.6303	0.4641	0.6375	0.4803	0.4667
THDv_bus L (%)	4.7073	4.3480	5.0503	5.4506	3.5467	4.3294	5.5762	3.0844
THDi_bus L (%)	5.7041	4.9754	4.7624	5.5527	3.0573	3.8728	5.7509	3.3106
THDv_bus M (%)	4.7636	3.7811	5.8248	5.1719	4.3853	5.6947	4.0420	3.2605
THDi_bus M (%)	3.6998	4.4071	4.2197	5.2719	5.1806	3.6974	4.8178	3.6766
Motor power factor	0.9133	0.9289	0.9146	0.9315	0.9322	0.9297	0.9592	0.9245
Reduction in KWh consumption (%)	16.7740	17.4464	17.1304	16.9247	17.4298	17.2816	17.6327	17.9605

(without the GP-SF-SS device), 0.06263 (constant gains controller), 0.03378 (ANN controller) and 0.04076 (FLC) to around 0.009344 (SOGA based tuned controller), 0.004511 (MOGA based tuned controller), 0.005837 (SOPSO) based tuned controller and 0.007559 (MOPSO based tuned controller). In addition the NMSE-ω_m of the SPIM motor is reduced from 0.5093 (without the GP-SF-SS device), 0.08417 (constant gains controller), 0.06218 (ANN controller) and 0.07776 (FLC) to around 0.007623 (SOGA based tuned controller), 0.005567 (MOGA based tuned controller), 0.8182 (SOPSO) based tuned controller and 0.007575 (MOPSO based tuned controller). The NMSE-I of the Motor current is reduced from 0.2398 (without the GP-SF-SS device), 0.01299 (constant gains controller), 0.02170 (ANN controller) and 0.04893 (FLC) to around 0.008792 (SOGA based tuned controller), 0.003647 (MOGA based tuned controller), 0.002873 (SOPSO) based tuned controller and 0.001690 (MOPSO based tuned controller). Total Harmonic Distortion (THD) (%) of the supply voltage is reduced from 17.486 (without the GP-SF-SS device), 6.6196 (constant gains controller), 8.0866 (ANN controller) and 8.4756 (FLC) to around 3.8914 (SOGA based tuned controller), 4.5209 (MOGA based tuned controller), 4.9241 (SOPSO) based tuned controller and 4.7073 (MOPSO based tuned controller). THD (%) of the supply current is reduced from 19.475 (without the GP-SF-SS device), 9.6328 (constant gains controller), 8.8441 (ANN controller) and 7.5479 (FLC) to around 5.2460 (SOGA based tuned controller), 3.6205 (MOGA based tuned controller), 5.8456 (SOPSO) based tuned controller and 5.7041 (MOPSO based tuned controller).

THD (%) of the motor voltage is reduced from 16.456 (without the GP-SF-SS device), 6.2423 (constant gains controller), 7.7610 (ANN controller) and 6.2888 (FLC) to around 3.0758 (SOGA based tuned controller), 5.4651 (MOGA based tuned controller), 4.4285 (SOPSO) based tuned controller and 4.7636 (MOPSO based tuned controller). THD (%) of the motor current is reduced from

18.465 (without the GP-SF-SS device), 8.2256 (constant gains controller), 8.4061 (ANN controller) and 9.3727 (FLC) to around 4.7253 (SOGA based tuned controller), 4.0933 (MOGA based tuned controller), 5.1721 (SOPSO) based tuned controller and 3.6998 (MOPSO based tuned controller). Motor power factor is improved from 0.7516 (without the GP-SF-SS device), 0.8950 (constant gains controller), 0.8909 (ANN controller) and 0.8837 (FLC) to around 0.9378 (SOGA based tuned controller), 0.9299 (MOGA based tuned controller), 0.9174 (SOPSO) based tuned controller and 0.9133 (MOPSO based tuned controller).

Reduction in KWh Consumption (%) is reduced from 0.000 (without the GP-SF-SS device), 13.8356 (constant gains controller), 13.6386 (ANN controller) and 13.2319 (FLC) to around 16.2601 (SOGA based tuned controller), 16.7016 (MOGA based tuned controller), 16.8207 (SOPSO) based tuned controller and 17.4587 (MOPSO based tuned controller).

Self tuned tan-sigmoid incremental integral action controller: Table 32 shows the system behavior using traditional controllers with constant controller gains for the (GP-SF-SS) eight schemes. In addition, Table 33 shows system behavior comparison using the SOGA based the self tuned tan-sigmoid incremental integral action controller and Table 34 shows the system behavior comparison using the MOGA based the self tuned tan-sigmoid incremental integral action controller.

Finally, Tables 35 and 36 show system behavior comparison using the SOPSO and MOPSO, respectively based the self tuned tan-sigmoid incremental integral action controller. Comparing the system dynamic response results of the two study cases, with GA and PSO tuning algorithms and traditional controllers with constant controller gains results, ANN controller and FLC, it is quite apparent that the GA and PSO tuning algorithms highly improved the system dynamic performance from a general power quality point of view. The GA and PSO tuning algorithms had a great impact on Motor RMS voltage (PU) is improved from 0.8782 (without the GP-SF-SS device), 0.9339 (constant gains controller), 0.9414 (ANN controller) and 0.9525 (FLC) to around 0.9878 (SOGA based tuned controller), 0.9923 (MOGA based tuned controller), 0.9798 (SOPSO) based tuned controller and 0.9831 (MOPSO based tuned controller). Motor RMS current (PU) is reduced from 0.8576 (without the GP-SF-SS device), 0.7141 (constant gains controller), 0.7269 (ANN controller) and 0.7158 (FLC) to around 0.5918 (SOGA based tuned controller), 0.6672 (MOGA based tuned controller), 0.6000 (SOPSO) based tuned controller and 0.6567 (MOPSO based tuned controller). Maximum Transient Motor Voltage Over/Under Shoot (PU) is reduced from 0.1597 (without the (GP-SF-SS) device), 0.0941 (constant gains controller), 0.0888 (ANN controller) and 0.0949 (FLC) to around 0.0485 (SOGA based tuned controller), 0.0380 (MOGA based tuned controller), 0.0484 (SOPSO) based tuned controller and 0.0482 (MOPSO based tuned controller). Maximum Transient Motor Current-Over/Under Shoot (PU) is reduced from 0.1775 (without the GP-SF-SS device), 0.0945 (constant gains controller), 0.0859 (ANN controller) and 0.0928 (FLC) to around 0.0221 (SOGA based tuned controller), 0.0434 (MOGA based tuned controller), 0.0293 (SOPSO) based tuned controller and 0.0279 (MOPSO based tuned controller). The system efficiency is improved from 0.8145 (without the GP-SF-SS device), 0.8585 (constant gains controller), 0.9012 (ANN controller) and 0.8788 (FLC) to around 0.9514 (SOGA based tuned controller), 0.9399

Table 32: System dynamic behavior comparison using the constant parameters tan-sigmoid incremental integral action controller

Items	GP-SF-SS scheme A	GP-SF-SS scheme B	GP-SF-SS scheme C	GP-SF-SS scheme D	GP-SF-SS scheme E	GP-SF-SS scheme F	GP-SF-SS scheme G	GP-SF-SS scheme H
RMS motor voltage (PU)	0.9339	0.9265	0.9458	0.9445	0.9545	0.9416	0.9370	0.9310
RMS motor current (PU)	0.7141	0.6575	0.6830	0.7139	0.6684	0.7152	0.6758	0.7117
Maximum transient voltage over/under shoot (PU)	0.0941	0.0899	0.0894	0.0913	0.0920	0.0942	0.0943	0.0911
Maximum transient current over/under shoot (PU)	0.0945	0.0909	0.0880	0.0921	0.0931	0.0932	0.0961	0.0942
System efficiency	0.8585	0.8803	0.8965	0.8646	0.8530	0.8597	0.8771	0.8985
NMSE_V $\times 10^{-1}$	0.7225	0.8596	0.3356	0.1378	0.6607	0.8153	0.7761	0.5173
NMSE_ω_m $\times 10^{-1}$	0.8313	0.3188	0.4275	0.9348	0.5120	0.5665	0.1580	0.6427
NMSE_I $\times 10^{-1}$	0.6793	0.7598	0.6881	0.3909	0.9516	0.5489	0.8092	0.4484
THDv_bus L (%)	9.7466	9.5541	9.6917	8.1775	9.6603	7.2400	7.0397	6.2557
THDi_bus L (%)	7.2956	7.1412	7.5625	6.1524	7.1222	6.8625	8.1881	9.3524
THDv_bus M (%)	6.9979	8.2872	8.0226	6.5162	6.0363	7.2690	7.4028	9.8268
THDi_bus M (%)	9.6199	7.6837	9.6028	7.9236	9.7389	9.6877	8.7807	8.5021
Motor power factor	0.8977	0.9048	0.8921	0.8989	0.8714	0.8899	0.8670	0.8938
Reduction in KWh consumption (%)	13.1976	12.8086	12.0070	12.3581	12.8105	13.9594	13.4968	12.5835

Table 33: System dynamic behavior comparison using the SOGA based tuned tan-sigmoid incremental integral action controller

Items	GP-SF-SS scheme A	GP-SF-SS scheme B	GP-SF-SS scheme C	GP-SF-SS scheme D	GP-SF-SS scheme E	GP-SF-SS scheme F	GP-SF-SS scheme G	GP-SF-SS scheme H
RMS motor voltage (PU)	0.9878	0.9900	0.9827	0.9752	0.9836	0.9905	0.9913	0.9939
RMS motor current (PU)	0.5918	0.6647	0.6432	0.6563	0.5988	0.6210	0.5873	0.6566
Maximum transient voltage over/under shoot (PU)	0.0485	0.0408	0.0234	0.0385	0.0328	0.0278	0.0269	0.0240
Maximum transient current over/under shoot (PU)	0.0221	0.0438	0.0224	0.0463	0.0317	0.0419	0.0488	0.0262
System efficiency	0.9514	0.9378	0.9464	0.9141	0.9296	0.9349	0.9171	0.9480
NMSE_V $\times 10^{-2}$	0.5229	0.7285	0.6060	0.3016	0.3046	0.4150	0.6596	0.6604
NMSE_ω_m $\times 10^{-2}$	0.1563	0.9586	0.4427	0.3670	0.3230	0.1548	0.5847	0.6571
NMSE_I $\times 10^{-2}$	0.2935	0.3050	0.1686	0.5785	0.4108	0.1625	0.6638	0.9420
THDv_bus L (%)	5.3448	5.3765	4.8314	3.4636	5.2365	5.0901	4.6188	5.0674
THDi_bus L (%)	3.2508	5.4138	5.0533	5.4832	5.4882	5.1754	4.9150	5.5726
THDv_bus M (%)	5.3376	3.2178	5.7244	3.9192	3.0366	5.1708	3.8947	5.0445
THDi_bus M (%)	5.2257	4.7685	4.8578	5.1605	3.4399	4.7170	5.5630	3.5081
Motor power factor	0.9164	0.9375	0.9567	0.9366	0.9437	0.9229	0.9393	0.9202
Reduction in KWh consumption (%)	16.7165	16.6108	16.7149	17.1051	17.4957	16.6504	17.7210	17.1739

Table 34: System dynamic behavior comparison using a selected solution from the MOGA Pareto front based tuned tan-sigmoid incremental integral ction controller

Items	GP-SF-SS scheme A	GP-SF-SS scheme B	GP-SF-SS scheme C	GP-SF-SS scheme D	GP-SF-SS scheme E	GP-SF-SS scheme F	GP-SF-SS scheme G	GP-SF-SS scheme H
RMS motor voltage (PU)	0.9923	0.9825	0.9877	0.9900	0.9790	0.9935	0.9867	0.9880
RMS motor current (PU)	0.6672	0.6120	0.5844	0.6480	0.6605	0.6058	0.6026	0.6639
Maximum transient voltage over/under shoot (PU)	0.0380	0.0463	0.0427	0.0324	0.0420	0.0264	0.0485	0.0273
Maximum transient current over/under shoot (PU)	0.0434	0.0389	0.0264	0.0227	0.0299	0.0489	0.0483	0.0282
System efficiency	0.9399	0.9300	0.9155	0.9259	0.9647	0.9323	0.9536	0.9580
NMSE_V $\times 10^{-2}$	0.5330	0.4638	0.9481	0.5785	0.6903	0.5463	0.8194	0.8086
NMSE_ω_m $\times 10^{-2}$	0.2997	0.1899	0.4980	0.7655	0.3363	0.9166	0.5075	0.5294
NMSE_I $\times 10^{-2}$	0.7327	0.8908	0.5843	0.4930	0.7583	0.7018	0.6255	0.2162
THDv_bus L (%)	4.0008	3.5197	3.2138	3.8968	3.9685	4.0856	5.7145	5.0560
THDi_bus L (%)	4.4022	4.4996	5.2333	4.6937	3.3793	3.3321	4.8964	5.8414
THDv_bus M (%)	3.0317	3.6635	5.7888	5.4573	3.0625	4.3955	4.1994	5.2075
THDi_bus M (%)	5.3838	5.7651	3.4035	3.7316	5.5952	4.9348	4.7840	4.4703
Motor power factor	0.9501	0.9617	0.9123	0.9428	0.9414	0.9485	0.9523	0.9556
Reduction in KWh consumption (%)	17.7517	17.2255	17.0292	17.8450	17.6869	17.3294	17.6795	17.3604

(MOGA based tuned controller), 0.9287 (SOPSO) based tuned controller and 0.9592 (MOPSO based tuned controller). Moreover, the Normalized Mean Square Error (NMSE-V) of the Motor voltage is reduced from 0.3293 (without the GP-SF-SS device), 0.07225 (constant gains controller), 0.03378 (ANN controller) and 0.04076 (FLC) to around 0.005229 (SOGA based tuned controller), 0.005330 (MOGA based tuned controller), 0.004453 (SOPSO) based tuned controller and 0.002398 (MOPSO based tuned controller). In addition the (NMSE-ω_m) of the SPIM motor is reduced from 0.5093 (without the (GP-SF-SS) device), 0.08313 (constant gains controller), 0.06218 (ANN controller) and 0.07776 (FLC) to around 0.001563 (SOGA based tuned controller), 0.002997 (MOGA based tuned controller), 0.3387 (SOPSO) based tuned controller and 0.008440 (MOPSO based tuned controller).

The NMSE-I of the motor current is reduced from 0.2398 (without the GP-SF-SS device), 0.06793 (constant gains controller), 0.02170 (ANN controller) and 0.04893 (FLC) to around 0.002935 (SOGA based tuned controller), 0.007327 (MOGA based tuned controller), 0.3279 (SOPSO) based tuned controller and 0.006582 (MOPSO based tuned controller).

Total Harmonic Distortion (THD) (%) of the supply voltage is reduced from 17.486 (without the GP-SF-SS device), 9.7466 (constant gains controller), 8.0866 (ANN controller) and 8.4756 (FLC) to around 5.3448 (SOGA based tuned controller), 4.0008 (MOGA based tuned controller), 4.1346 (SOPSO) based tuned controller and 5.0450 (MOPSO based tuned controller). THD (%) of the supply current is reduced from 19.475 (without the GP-SF-SS device), 7.2956 (constant gains controller), 8.8441 (ANN controller) and 7.5479 (FLC) to around 3.2508 (SOGA based tuned controller), 4.4022 (MOGA based tuned controller), 5.8108 (SOPSO) based tuned controller and 3.2818 (MOPSO based tuned controller). THD (%) of the motor voltage is reduced from 16.456 (without the GP-SF-SS device), 6.9979 (constant gains controller), 7.7610

Table 35: System dynamic behavior comparison using the SOPSO based tuned tan-sigmoid incremental integral action controller

Items	GP-SF-SS scheme A	GP-SF-SS scheme B	GP-SF-SS scheme C	GP-SF-SS scheme D	GP-SF-SS scheme E	GP-SF-SS scheme F	GP-SF-SS scheme G	GP-SF-SS scheme H
RMS motor voltage (PU)	0.9798	0.9863	0.9941	0.9819	0.9884	0.9830	0.9879	0.9893
RMS motor current (PU)	0.6000	0.6433	0.6270	0.6640	0.6442	0.6005	0.6205	0.5955
Maximum transient voltage over/under shoot (PU)	0.0484	0.0255	0.0238	0.0253	0.0265	0.0472	0.0256	0.0390
Maximum transient current over/under shoot (PU)	0.0293	0.0280	0.0417	0.0371	0.0480	0.0310	0.0415	0.0481
System efficiency	0.9287	0.9221	0.9242	0.9235	0.9161	0.9184	0.9404	0.9484
NMSE_V $\times 10^{-2}$	0.4453	0.6888	0.7994	0.1934	0.3481	0.1419	0.4995	0.5662
NMSE_ω_m $\times 10^{-2}$	0.3387	0.1995	0.5803	0.9102	0.2344	0.5724	0.2868	0.6031
NMSE_I $\times 10^{-2}$	0.3279	0.6662	0.1176	0.1213	0.7383	0.1976	0.7731	0.7481
THDv_bus L (%)	4.1346	5.7415	3.1070	5.7188	5.0420	4.8502	4.2849	3.5157
THDi_bus L (%)	5.8108	5.5253	4.1667	4.7953	4.1119	5.4194	4.5117	5.3050
THDv_bus M (%)	3.7638	4.0936	3.9757	3.9115	5.7001	4.5352	5.0069	5.4963
THDi_bus M (%)	5.1561	3.6952	5.6887	3.2725	4.5574	5.5767	5.4575	4.8076
Motor power factor	0.9483	0.9636	0.9267	0.9211	0.9608	0.9257	0.9318	0.9461
Reduction in KWh consumption (%)	16.4160	17.4049	16.6372	17.1205	16.3299	17.4366	16.7901	17.7645

Table 36: System dynamic behavior comparison using a selected solution from the MOPSO Pareto front based tuned tan-sigmoid incremental integral ction controller

Items	GP-SF-SS scheme A	GP-SF-SS scheme B	GP-SF-SS scheme C	GP-SF-SS scheme D	GP-SF-SS scheme E	GP-SF-SS scheme F	GP-SF-SS scheme G	GP-SF-SS scheme H
RMS motor voltage (PU)	0.9831	0.9835	0.9884	0.9922	0.9826	0.9837	0.9872	0.9866
RMS motor current (PU)	0.6567	0.6484	0.6655	0.6302	0.5813	0.6337	0.6535	0.6679
Maximum transient voltage over/under shoot (PU)	0.0482	0.0445	0.0477	0.0305	0.0293	0.0368	0.0264	0.0277
Maximum transient current over/under shoot (PU)	0.0279	0.0400	0.0233	0.0282	0.0404	0.0305	0.0304	0.0419
System efficiency	0.9592	0.9645	0.9331	0.9300	0.9287	0.9312	0.9446	0.9436
NMSE_V $\times 10^{-2}$	0.2398	0.1248	0.1557	0.4391	0.4864	0.1424	0.8244	0.7792
NMSE_ω_m $\times 10^{-2}$	0.8440	0.7200	0.6191	0.7520	0.2874	0.1927	0.3002	0.2484
NMSE_I $\times 10^{-2}$	0.6582	0.6585	0.3243	0.2198	0.8071	0.6359	0.5505	0.1174
THDv_bus L (%)	5.0450	3.1221	5.7919	4.4286	5.0034	5.2930	4.4829	4.4434
THDi_bus L (%)	3.2818	4.7248	5.3759	3.8518	4.3383	3.1506	3.2643	4.4729
THDv_bus M (%)	4.4262	3.0417	3.9160	5.1100	5.2568	4.1538	4.1527	3.7336
THDi_bus M (%)	4.8837	3.0255	5.7988	4.1878	4.0048	4.9113	4.2765	5.3969
Motor power factor	0.9318	0.9392	0.9594	0.9459	0.9227	0.9155	0.9544	0.9343
Reduction in KWh consumption (%)	17.4029	16.7924	17.7075	17.0419	17.4600	16.8923	16.6409	16.4083

(ANN controller) and 6.2888 (FLC) to around 5.3376 (SOGA based tuned controller), 3.0317 (MOGA based tuned controller), 3.7638 (SOPSO) based tuned controller and 4.4262 (MOPSO based tuned controller). THD (%) of the motor current is reduced from 18.465 (without the GP-SF-SS device), 9.6199 (constant gains controller), 8.4061 (ANN controller) and 9.3727 (FLC) to around 5.2257 (SOGA based tuned controller), 5.3838 (MOGA based tuned controller), 5.1561 (SOPSO) based tuned controller and 4.8837 (MOPSO based tuned controller). Motor power factor is improved from 0.7516 (without the GP-SF-SS device), 0.8977 (constant gains controller), 0.8909 (ANN controller) and 0.8837 (FLC) to around 0.9164 (SOGA based tuned controller), 0.9501 (MOGA based tuned controller), 0.9483 (SOPSO) based tuned controller and 0.9318 (MOPSO based tuned controller).

Reduction in KWh Consumption (%) is reduced from 0.000 (without the GP-SF-SS device), 12.1976 (constant gains controller), 13.6386 (ANN controller) and 13.2319 (FLC) to around 17.9799 (SOGA based tuned controller), 17.6391 (MOGA based tuned controller), 17.5938 (SOPSO) based tuned controller and 17.8238 (MOPSO based tuned controller).

Self tuned multi-stage incremental action controller: Table 37 shows the system behavior using traditional controllers with constant controller gains for the (GP-SF-SS) eight schemes. In addition, Table 38 shows system behavior comparison using the SOGA based the self tuned multi-stage incremental action controller and Table 39 shows the system behavior comparison using the MOGA based the self tuned multi-stage incremental action controller. Finally, Table 40 and 41 show system behavior comparison using the SOPSO and MOPSO respectively based the self tuned multi-stage incremental action controller. Comparing the system dynamic response results of the two study cases with GA and PSO tuning algorithms and traditional controllers with

Table 37: System dynamic behavior comparison using the constant parameters multi-stage incremental action controller

Items	GP-SF-SS scheme A	GP-SF-SS scheme B	GP-SF-SS scheme C	GP-SF-SS scheme D	GP-SF-SS scheme E	GP-SF-SS scheme F	GP-SF-SS scheme G	GP-SF-SS scheme H
RMS motor voltage (PU)	0.9465	0.9403	0.9483	0.9397	0.9306	0.9460	0.9545	0.9492
RMS motor current (PU)	0.7031	0.6988	0.7068	0.7489	0.6859	0.6922	0.6823	0.6932
Maximum transient voltage over/under shoot (PU)	0.0938	0.0952	0.0966	0.0913	0.0927	0.0944	0.0907	0.0915
Maximum transient current over/under shoot (PU)	0.0877	0.0872	0.0882	0.0869	0.0873	0.0908	0.0944	0.0889
System efficiency	0.8628	0.8747	0.8853	0.8816	0.8649	0.8867	0.8589	0.8791
NMSE_V $\times 10^{-1}$	0.1334	0.8238	0.2414	0.8787	0.8119	0.5822	0.9541	0.5921
NMSE_ω_m $\times 10^{-1}$	0.9611	0.9203	0.2588	0.4302	0.4102	0.8110	0.7654	0.6572
NMSE_I $\times 10^{-1}$	0.7236	0.8603	0.8733	0.8893	0.6823	0.6743	0.1716	0.6206
THDv_bus L (%)	9.3237	6.1402	7.4224	6.3810	7.3028	6.0499	9.1435	6.1176
THDi_bus L (%)	7.6456	6.1512	8.6122	7.2772	8.1657	7.6479	6.5964	6.2682
THDv_bus M (%)	8.3815	8.4296	6.6980	7.5833	8.7248	7.6670	6.8293	8.2841
THDi_bus M (%)	9.2265	9.4221	9.4118	9.7077	8.9679	7.4303	6.2827	6.4387
Motor power factor	0.8664	0.8831	0.8661	0.8935	0.8598	0.8929	0.8795	0.8830
Reduction in KWh consumption (%)	12.0813	12.6022	12.9933	13.1296	12.4333	13.6200	13.0986	12.3687

Table 38: System dynamic behavior comparison using the SOGA based tuned multi-stage incremental action controller

Items	GP-SF-SS scheme A	GP-SF-SS scheme B	GP-SF-SS scheme C	GP-SF-SS scheme D	GP-SF-SS scheme E	GP-SF-SS scheme F	GP-SF-SS scheme G	GP-SF-SS scheme H
RMS motor voltage (PU)	0.9894	0.9849	0.9773	0.9886	0.9825	0.9779	0.9866	0.9919
RMS motor current (PU)	0.6446	0.6312	0.6215	0.6201	0.5879	0.6199	0.6130	0.6072
Maximum transient voltage over/under shoot (PU)	0.0300	0.0246	0.0329	0.0311	0.0481	0.0452	0.0290	0.0231
Maximum transient current over/under shoot (PU)	0.0220	0.0378	0.0425	0.0443	0.0396	0.0288	0.0259	0.0400
System efficiency	0.9221	0.9475	0.9324	0.9156	0.9480	0.9573	0.9170	0.9327
NMSE_V $\times 10^{-2}$	0.7376	0.5544	0.8761	0.8761	0.4977	0.4506	0.6239	0.9361
NMSE_ω_m $\times 10^{-2}$	0.8525	0.7383	0.4283	0.8241	0.5473	0.8922	0.2278	0.4722
NMSE_I $\times 10^{-2}$	0.8973	0.8664	0.7651	0.1978	0.4379	0.2272	0.8348	0.1598
THDv_bus L (%)	5.2884	3.6051	5.2068	5.4897	5.3050	5.1615	5.5799	4.2124
THDi_bus L (%)	3.8367	5.0997	4.4273	3.1765	3.5628	5.0708	5.7752	5.0140
THDv_bus M (%)	4.6016	5.2352	3.4199	4.5988	3.6028	5.4552	3.7496	3.8070
THDi_bus M (%)	5.7616	5.3605	3.3849	5.4036	5.2543	3.9970	5.1102	3.1901
Motor power factor	0.9648	0.9176	0.9361	0.9189	0.9492	0.9281	0.9153	0.9211
Reduction in KWh consumption (%)	16.9674	16.8716	17.7366	17.0871	16.4346	17.3845	17.7203	16.0644

Table 39: System dynamic behavior comparison using a selected solution from the MOGA Pareto front based tuned Multi-Stage Incremental action ontroller

Items	GP-SF-SS scheme A	GP-SF-SS scheme B	GP-SF-SS scheme C	GP-SF-SS scheme D	GP-SF-SS scheme E	GP-SF-SS scheme F	GP-SF-SS scheme G	GP-SF-SS scheme H
RMS motor voltage (PU)	0.9888	0.9955	0.9947	0.9762	0.9824	0.9862	0.9804	0.9872
RMS motor current (PU)	0.6226	0.6613	0.6206	0.6524	0.6546	0.5950	0.6155	0.6269
Maximum transient voltage over/under shoot (PU)	0.0274	0.0406	0.0476	0.0314	0.0384	0.0390	0.0220	0.0492
Maximum transient current over/under shoot (PU)	0.0469	0.0411	0.0341	0.0414	0.0388	0.0302	0.0457	0.0250
System efficiency	0.9344	0.9149	0.9542	0.9416	0.9528	0.9647	0.9166	0.9502
NMSE_V $\times 10^{-2}$	0.4401	0.3441	0.7284	0.5516	0.5401	0.2528	0.6967	0.6146
NMSE_ω_m $\times 10^{-2}$	0.5495	0.6575	0.6114	0.1795	0.9326	0.1501	0.5793	0.8413
NMSE_I $\times 10^{-2}$	0.2884	0.1171	0.4845	0.2851	0.1622	0.8887	0.9037	0.8336
THDv_bus L (%)	4.9745	4.4705	5.8253	3.5424	4.6025	4.3991	4.1459	4.4155
THDi_bus L (%)	5.2901	4.2462	3.7039	4.8165	4.0602	4.2419	3.8756	4.2440
THDv_bus M (%)	5.3575	3.9766	3.5799	4.4642	3.6154	4.6619	5.7909	4.3428
THDi_bus M (%)	3.2045	3.3622	3.1048	5.4684	4.1931	5.2613	5.3305	4.1397
Motor power factor	0.9551	0.9377	0.9180	0.9195	0.9535	0.9261	0.9414	0.9191
Reduction in KWh consumption (%)	16.4267	17.2462	16.5753	16.4269	16.0555	17.5355	16.9251	17.9098

constant controller gains results, ANN controller and FLC, it is quite apparent that the GA and PSO tuning algorithms highly improved the system dynamic performance from a general power quality point of view. The GA and PSO tuning algorithms had a great impact on motor RMS voltage (PU) is improved from 0.8782 (without the GP-SF-SS device), 0.9465 (constant gains controller), 0.9414 (ANN controller) and 0.9525 (FLC) to around

Table 40: System dynamic behavior comparison using the SOPSO based tuned multi-stage incremental action controller

Items	GP-SF-SS scheme A	GP-SF-SS scheme B	GP-SF-SS scheme C	GP-SF-SS scheme D	GP-SF-SS scheme E	GP-SF-SS scheme F	GP-SF-SS scheme G	GP-SF-SS scheme H
RMS motor voltage (PU)	0.9760	0.9867	0.9894	0.9947	0.9904	0.9902	0.9839	0.9880
RMS motor current (PU)	0.5813	0.6398	0.6452	0.6053	0.6036	0.6438	0.6505	0.6688
Maximum transient voltage over/under shoot (PU)	0.0296	0.0373	0.0354	0.0483	0.0283	0.0352	0.0365	0.0439
Maximum transient current over/Under shoot (PU)	0.0272	0.0472	0.0475	0.0222	0.0432	0.0482	0.0445	0.0476
System efficiency	0.9638	0.9342	0.9637	0.9394	0.9407	0.9320	0.9570	0.9408
NMSE_V $\times 10^{-2}$	0.4588	0.3869	0.6361	0.6242	0.9130	0.3472	0.8454	0.5022
NMSE_ω_m $\times 10^{-2}$	0.6239	0.7875	0.6591	0.7100	0.6362	0.6990	0.7834	0.9236
NMSE_I $\times 10^{-2}$	0.8869	0.8738	0.6364	0.2293	0.8519	0.4789	0.7844	0.9172
THDv_bus L (%)	4.9696	3.9434	5.6327	5.1629	4.1561	3.5764	4.1538	3.4587
THDi_bus L (%)	3.7954	5.6413	3.6857	3.3838	4.1887	4.8167	3.5352	4.1621
THDv_bus M (%)	4.5814	3.6308	4.9037	3.8953	4.3503	4.4522	4.9685	3.5672
THDi_bus M (%)	3.7586	3.6731	4.5067	4.6073	5.3577	3.8376	3.7365	3.7012
Motor power factor	0.9598	0.9397	0.9474	0.9478	0.9625	0.9450	0.9362	0.9463
Reduction in KWh consumption (%)	16.8547	17.8326	16.1417	16.7385	17.6698	16.0446	16.3056	16.4348

Table 41: System dynamic behavior comparison using a selected solution from the MOPSO Pareto front based tuned multi-stage incremental ction ontroller

Items	GP-SF-SS scheme A	GP-SF-SS scheme B	GP-SF-SS scheme C	GP-SF-SS scheme D	GP-SF-SS scheme E	GP-SF-SS scheme F	GP-SF-SS scheme G	GP-SF-SS scheme H
RMS motor voltage (PU)	0.9915	0.9767	0.9944	0.9938	0.9873	0.9802	0.9929	0.9855
RMS motor current (PU)	0.6057	0.6155	0.6253	0.6450	0.6076	0.5901	0.6199	0.6220
Maximum transient voltage over/under shoot (PU)	0.0281	0.0471	0.0221	0.0382	0.0369	0.0400	0.0306	0.0283
Maximum transient current over/under shoot (PU)	0.0334	0.0302	0.0406	0.0480	0.0314	0.0375	0.0252	0.0266
System efficiency	0.9271	0.9238	0.9433	0.9418	0.9578	0.9235	0.9279	0.9430
NMSE_V $\times 10^{-2}$	0.7217	0.4314	0.6061	0.8761	0.7558	0.1252	0.5398	0.7257
NMSE_ω_m $\times 10^{-2}$	0.3437	0.7327	0.7851	0.8464	0.1876	0.2789	0.9443	0.8082
NMSE_I $\times 10^{-2}$	0.7074	0.2361	0.7185	0.5610	0.8967	0.2983	0.5994	0.2509
THDv_bus L (%)	3.1842	3.8447	4.9337	5.7144	3.1357	5.3452	3.6542	5.8488
THDi_bus L (%)	5.2700	3.0767	5.7271	5.4394	5.8110	3.7308	4.3863	3.9398
THDv_bus M (%)	3.8515	3.2479	5.6469	3.4935	4.1156	4.3962	5.3149	4.1691
THDi_bus M (%)	5.6710	4.4670	3.6193	4.2127	5.3676	3.4247	3.9314	5.3348
Motor power factor	0.9394	0.9193	0.9286	0.9576	0.9349	0.9150	0.9589	0.9255
Reduction in KWh consumption (%)	17.2697	17.6268	17.8896	17.5181	16.3812	16.8454	17.9172	17.8797

0.9894 (SOGA based tuned controller), 0.9888 (MOGA based tuned controller), 0.9760 (SOPSO) based tuned controller and 0.9915 (MOPSO based tuned controller). Motor RMS current (PU) is reduced from 0.8576 (without the GP-SF-SS device), 0.7031 (constant gains controller), 0.7269 (ANN controller) and 0.7158 (FLC) to around 0.6446 (SOGA based tuned controller), 0.6226 (MOGA based tuned controller), 0.5813 (SOPSO) based tuned controller and 0.6057 (MOPSO based tuned controller). Maximum Transient Motor Voltage Over/Under Shoot (PU) is reduced from 0.1597 (without the (GP-SF-SS) device), 0.0938 (constant gains controller), 0.0888 (ANN controller) and 0.0949 (FLC) to around 0.0300 (SOGA based tuned controller), 0.0274 (MOGA based tuned controller), 0.0296 (SOPSO) based tuned controller and 0.0281 (MOPSO based tuned controller). Maximum transient motor current-over/under shoot (PU) is reduced from 0.1775 (without the GP-SF-SS device), 0.0877 (constant gains controller), 0.0859 (ANN controller) and 0.0928 (FLC) to around 0.0220 (SOGA based tuned controller), 0.0469 (MOGA based tuned controller), 0.0272 (SOPSO) based tuned controller and 0.0334 (MOPSO based tuned controller). The system efficiency is improved from 0.8145 (without the GP-SF-SS device), 0.8628 (constant gains controller), 0.9012 (ANN controller) and 0.8788 (FLC) to around 0.9221 (SOGA based tuned controller), 0.9344 (MOGA based tuned controller), 0.9638 (SOPSO) based tuned controller and 0.9271 (MOPSO based tuned controller). Moreover, the Normalized Mean Square Error (NMSE-V) of the Motor voltage is reduced from 0.3293 (without the GP-SF-SS device), 0.01334 (constant gains controller), 0.03378 (ANN controller) and 0.04076 (FLC) to around 0.007376 (SOGA based tuned controller), 0.004401 (MOGA based tuned controller), 0.004588 (SOPSO) based tuned controller and 0.007217 (MOPSO based tuned controller). In addition, the (NMSE-ω_m) of the SPIM motor is reduced from 0.5093 (without the GP-SF-SS device), 0.09611 (constant gains controller), 0.06218 (ANN controller) and 0.07776 (FLC) to around 0.008525 (SOGA based tuned controller), 0.005495 (MOGA based tuned controller), 0.006239 (SOPSO) based

tuned controller and 0.003437 (MOPSO based tuned controller). The (NMSE-I) of the Motor current is reduced from 0.2398 (without the GP-SF-SS device), 0.07236 (constant gains controller), 0.02170 (ANN controller) and 0.04893 (FLC) to around 0.008973 (SOGA based tuned controller), 0.002884 (MOGA based tuned controller), 0.008869 (SOPSO) based tuned controller and 0.007074 (MOPSO based tuned controller).

Total Harmonic Distortion THD (%) of the supply voltage is reduced from 17.486 (without the GP-SF-SS device), 9.3237 (constant gains controller), 8.0866 (ANN controller) and 8.4756 (FLC) to around 5.2884 (SOGA based tuned controller), 4.9745 (MOGA based tuned controller), 4.9696 (SOPSO) based tuned controller and 3.1842 (MOPSO based tuned controller). THD (%) of the supply current is reduced from 19.475 (without the GP-SF-SS device), 7.6456 (constant gains controller), 8.8441 (ANN controller) and 7.5479 (FLC) to around 3.8367 (SOGA based tuned controller), 5.2901 (MOGA based tuned controller), 3.7954 (SOPSO) based tuned controller and 5.2700 (MOPSO based tuned controller). THD (%) of the motor voltage is reduced from 16.456 (without the GP-SF-SS device), 8.3815 (constant gains controller), 7.7610 (ANN controller) and 6.2888 (FLC) to around 4.6016 (SOGA based tuned controller), 5.3575 (MOGA based tuned controller), 4.5814 (SOPSO) based tuned controller and 3.8515 (MOPSO based tuned controller). THD (%) of the motor current is reduced from 18.465 (without the GP-SF-SS device), 9.2265 (constant gains controller), 8.4061 (ANN controller) and 9.3727 (FLC) to around 5.7616 (SOGA based tuned controller), 3.2045 (MOGA based tuned controller), 3.7586 (SOPSO) based tuned controller and 5.6710 (MOPSO based tuned controller). Motor power factor is improved from 0.7516 (without the GP-SF-SS device), 0.8664 (constant gains controller), 0.8909 (ANN controller) and 0.8837 (FLC) to around 0.9648 (SOGA based tuned controller), 0.9551 (MOGA based tuned controller), 0.9598 (SOPSO) based tuned controller and 0.9394 (MOPSO based tuned controller).

Reduction in KWh Consumption (%) is reduced from 0.000 (without the GP-SF-SS device), 12.0813 (constant gains controller), 12.6386 (ANN controller) and 12.2319 (FLC) to around 16.0901 (SOGA based tuned controller), 17.6541 (MOGA based tuned controller), 16.6020 (SOPSO) based tuned controller and 17.6654 (MOPSO based tuned controller).

CONCLUSION

The study presents a family of novel low cost Green Plug electricity saving device/Smart Filter/Soft Starter (GP-SF-SS) devices developed by the First researcher and equipped with a dynamic online error driven optimally tuned controller using a dynamic online error driven optimally tuned controllers.

The GP-SF-SS are a small low cost energy conservation devices in the form add-on dynamic switched capacitor filter compensator schemes for low horse power motors used in household appliances, washers, dryers, fans, water pumps, ventilation systems, air-conditioners and other cyclical motorized loads used in dispersing machines, actuators and small converters with induction motor size up to 5 KVA. The GP-SF-SS device uses a smart dynamic error driven tracking controller to ensure combined functions of speed reference tracking and efficient utilization. This ensures of reduced electricity consumption, efficient operation, reduced motor losses, motor extended life span, enhanced AC supply operation with minimal voltage and current excursions, harmonics, voltage sags, inrush currents and severe excursions that cause voltage flickering, notching and spikes.

The GP-SF-SS devices family can be used with all types of small horse power motors with speed control up to 5 KVA with billions of small motors used in multitude of applications that consumes over 50-60% of total electrical energy generated in the world. The GP-SF-SS device can save 10-20% of the electricity cost of operating the small motor over the estimated motor life span of 7-10 years. This translate into millions of dollars in daily electricity savings, reduced electrical utility overloading conditions, blackouts, brownouts and enhanced secure and reliable operation with additional sizable power capacity release due to reduced electric demand and feeder losses.

APPENDIX

SPIM: Nominal Power = 0.25 HP, Nominal voltage = 110 V, Nominal frequency = 60 HZ, Main Winding Stator: RS = 2.02 Ohm, Lls = 7.4 mH, Main winding rotor: Rr ′= 4.12 ohm, Llr ′= 5.6 mH, Main winding mutual inductance: Lms = 0.177 H, Auxilary Winding Stator: RS = 7.14 Ohm, Lls = 8.54 mH, Inertia: J = 0.0146, Pairs of poles: P = 2, ratio of turns:1.18, Capacitor start: Rst = 2.15 ohm, Cst = 255 μf, Capacitor Run: Rru=18 ohm, Cru = 21.1 μF.

GPFC-Scheme A: R_f = 0.2 Ω, L_f = 2 mH, C_f = 35 μF, C_p = 100 μF,

GPFC-Scheme B: R_f = 0.3 Ω, L_f = 5 mH, C_f = 45 μF, C_p = 120 μF,

GPFC-Scheme C: R_f = 0.25 Ω, L_f = 3 mH, C_f = 25 μF, C_p = 90 μF,

GPFC-Scheme D: R_f = 0.25 Ω, L_f = 4 mH, C_f =55 μF, C_s = 25 μF,

GPFC-Scheme E: C_f = 65 μF, C_s = 35 μF,

GPFC-Scheme F: $R_1 = 0.3\ \Omega$, $L_1 = 5$ mH, $C_1 = 75\ \mu$F, $R_2 = 0.2\ \Omega$, $L_2 = 3$ mH, $C_2 = 100\ \mu$F,
GPFC-Scheme G: $R_1 = 0.5\ \Omega$, $L_1 = 3$ mH, $C_1 = 85\ \mu$F,
GPFC-Scheme H: $R_1 = 0.4\ \Omega$, $C_1 = 85\ \mu$F, $R_2 = 0.3\ \Omega$, $L_2 = 4$ mH, $C_2 = 120\ \mu$F,
Control Weightings Scaling: $\gamma_{vs} = 0.86$, $\gamma_{Is} = 0.45$, $\gamma_{Ps} = 0.25$, $\gamma_{vm} = 0.92$, $\gamma_{Im} = 0.54$, $\gamma_{Pm} = 0.24$,
Tuned conventional PID controller Gains: $10 \le K_{Ps}, K_{Pm} \le 200$, $1 \le K_{Is}, K_{Im} \le 20$, $0.1 \le K_{Ds}, K_{Dm} \le 10$,
Tuned modified PID controller- I Gains: $50 \le K_{Ps}, K_{Pm} \le 300$, $1 \le K_{Is}, K_{Im} \le 10$, $0.1 \le K_{Ds}, K_{Dm} \le 5$, $1 \le K_{es}, K_{em} \le 50$,
Tuned modified PID controller -II Gains: $50 \le K_{Ps}, K_{Pm} \le 300$, $1 \le K_{Is}, K_{Im} \le 10$, $0.1 \le K_{Ds}, K_{Dm} \le 5$, $1 \le K_{es}, K_{em} \le 100$,
Tuned Variable structure sliding mode controller VSC/SMC/B-B Gains: $1 \le \beta_{0s}$, $\beta_{0m} \le 10$, $1 \le \beta_{1s}, \beta_{1m} \le 50$, $0.01 \le K_{\alpha s}, K_{\alpha m} \le 1$
Tuned Zonal Activation or Target Practice Controller Gains: $1 \le \beta_{0s}, \beta_{0m} \le 10$, $0 \le \beta_{1s}$, $\beta_{1m} \le 50$, $0.01 \le K_{\alpha s}, K_{\alpha m} \le 1$
Tuned Tan-sigmoid Incremental Integral Action Controller Gains: $1 \le \beta_{0s}, \beta_{0m} \le 5$, $50 \le K_{0s}, K_{0m} \le 200$
Tuned Multi-Stage Incremental Action Controller Gains: $1 \le \gamma_{1s}, \gamma_{1m} \le 100$, $1 \le \gamma_{2s}, \gamma_{2m} \le 100$, $1 \le \gamma_{3s}, \gamma_{3m} \le 100$, $1 \le \gamma_{4s}, \gamma_{4m} \le 100$

REFERENCES

Berizzi, A., M. Innorta and P. Marannino, 2001. Multiobjective optimization techniques applied to modern power systems. IEEE Power Eng. Soc. Winter Meeting, 3: 1503-1508.

Coello, C.A.C. and M.S. Lechuga, 2002. MOPSO: A proposal for multiple objective particle swarm optimization. Proceedings of the 2002 Congress on Evolutionary Computation part of the 2002 IEEE World Congress on Computational Intelligence, May, 12-17, Hawaii, pp: 1051-1056.

Davis, L., 1991. Handbooks of Genetic Algorithm. Van Nostrand Reinhold Co., New York.

De Rossiter Correa, M.B., C.B. Jacobina, E.R.C. da Silva and A.M.N. Lima, 2004. Vector control strategies for single-phase induction motor drive systems. IEEE Trans. Ind. Electr., 51: 1073-1080.

Deb, K., A. Pratap, S. Agarwal and T. Meyarivan, 2002. A fast and elitist multiobjective genetic algorithm: NSGA-II. IEEE Tran. Evol. Comput., 6: 182-197.

Kennedy, J. and R. Eberhart, 1995. Particle swarm optimization. Proc. IEEE Int. Conf. Neural Networks, 4: 1942-1948.

Mademlis, C., I. Kioskeridis and T. Theodoulidis, 2005. Optimization of single-phase induction Motors-part I: Maximum energy efficiency control. IEEE Trans. Energy Convers., 20: 187-195.

Neri, A.L., A.C.C. Lyra and Y. Burian, 2005. New topology supply for the single-phase induction motor: A simple soft starter. Power Tech, 2005 IEEE Russia, pp: 1-8.

Ngatchou, P., A. Zarei and A. El-Sharkawi, 2005. Pareto multi objective optimization. Proceedings of the 13th International Conference on Intelligent Systems Application to Power Systems, Nov. 6-10, Arlington, VA., pp: 84-91.

Poirier, E., M. Ghribi and A. Kaddouri, 2001. Losses minimization control of induction motor drives based on genetic algorithms. Electric Machines Drives Conf., 2001: 475-478.

Sharaf, A.M. and A. Aljankawey, 2006. Voltage stabilization using a facts modulated power filter. IEEE Int. Symp. Ind. Electronics, 3: 1937-1942.

Sharaf, A.M. and P. Kreidi, 2002. Dynamic compensation using switched/modulated power filters. Can. Conf. Electrical Comput. Eng., 1: 230-235.

Sharaf, A.M. and R. Chalet, 1998. A low cost on-off modulated power filter for single phase motorized loads. IEEE Can. Conf. Electrical Comput. Eng., 2: 862-865.

Sharaf, A.M., C. Guo and H. Huang, 2000. A smart PWM switched power filter for single phase nonlinear loads. Can. Conf. Electrical Comput. Eng., 2: 932-935.

Sharaf, A.M., Guo, C. and H. Huang, 1998. A smart PWM-modulated power filter for single phase motorized loads. IEEE Can. Conf. Electrical Comput. Eng., 2: 778-781.

Shenoy, T.P. and J.S. Nirody, 2006. Design and development of a high performance electronic starter for single-phase induction motors. Proceedings of the International Conference on Power Electronics, Dec. 1-5, Drives and Energy Systems, pp: 12-15.

Shi, Y. and R.C. Eberhart, 1999. Empirical study of particle swarm optimization. Proceeding of the IEEE International Conference on Evolutionary Computer, July 6-9, Washington, DC., USA., pp: 1945-1950.

Srinivas, N. and K. Deb, 1994. Multiobjective optimization using nondominated sorting in genetic algorithms. Evolut. Comput., 2: 221-248.

Zahedi, B. and S. Vaez-Zadeh, 2009. Efficiency optimization control of single-phase induction motor drives. IEEE Trans. Power Electr., 24: 1062-1070.